

Small Molecule Antagonist of Leukocyte Function Associated Antigen-1 (LFA-1): Structure–Activity Relationships Leading to the Identification of 6-((5*S*,9*R*)-9-(4-Cyanophenyl)-3-(3,5-dichlorophenyl)-1-methyl-2,4-dioxo-1,3,7-triazaspiro[4.4]nonan-7-yl)nicotinic Acid (BMS-688521)[†]

Scott H. Watterson,^{*,‡} Zili Xiao,[‡] Dharmpal S. Dodd,[‡] David R. Tortolani,[‡] Wayne Vaccaro,[‡] Dominique Potin,[§] Michele Launay,[§] Dawn K. Stetsko,[‡] Stacey Skala,[‡] Patric M. Davis,[‡] Deborah Lee,[‡] Xiaoxia Yang,[‡] Kim W. McIntyre,[‡] Praveen Balimane,[‡] Karishma Patel,[‡] Zheng Yang,[‡] Punit Marathe,[‡] Pathanjali Kadiyala,[‡] Andrew J. Tebben,[‡] Steven Sheriff,[‡] ChiehYing Y. Chang,[‡] Theresa Ziemba,[‡] Huiping Zhang,[‡] Bang-Chi Chen,[‡] Albert J. DelMonte,[‡] Nelly Aranibar,[‡] Murray McKinnon,[‡] Joel C. Barrish,[‡] Suzanne J. Suchard,[‡] and T. G. Murali Dhar[‡]

[‡]Bristol-Myers Squibb Research and Development, P.O. Box 4000, Princeton, New Jersey 08543, and [§]Cerep, 19 Avenue du Quebec, 91951 Courtaboeuf cedex, France

Received March 16, 2010

Leukocyte function-associated antigen-1 (LFA-1), also known as CD11a/CD18 or $\alpha_L\beta_2$, belongs to the β_2 integrin subfamily and is constitutively expressed on all leukocytes. The major ligands of LFA-1 include three intercellular adhesion molecules 1, 2, and 3 (ICAM 1, 2, and 3). The interactions between LFA-1 and the ICAMs are critical for cell adhesion, and preclinical animal studies and clinical data from the humanized anti-LFA-1 antibody efalizumab have provided proof-of-concept for LFA-1 as an immunological target. This article will detail the structure–activity relationships (SAR) leading to a novel second generation series of highly potent spirocyclic hydantoin antagonists of LFA-1. With significantly enhanced in vitro and ex vivo potency relative to our first clinical compound (1), as well as demonstrated in vivo activity and an acceptable pharmacokinetic and safety profile, 6-((5*S*,9*R*)-9-(4-cyanophenyl)-3-(3,5-dichlorophenyl)-1-methyl-2,4-dioxo-1,3,7-triazaspiro-[4.4]nonan-7-yl)nicotinic acid (2e) was selected to advance into clinical trials.

Introduction

Integrins are a family of α/β heterodimeric receptors that mediate cell–cell and cell–extracellular interactions.¹ Leukocyte function-associated antigen-1 (LFA-1^a), also known as CD11a/CD18 or $\alpha_L\beta_2$, belongs to the β_2 integrin subfamily and is constitutively expressed on all leukocytes.¹ The major ligands of LFA-1 include three members of the immunoglobulin super gene family, intercellular adhesion molecules 1, 2, and 3 (ICAM 1, 2, and 3). In particular, the interaction between LFA-1 and ICAM-1 promotes tight adhesion between many cell types including endothelial cells as well as other leukocytes and plays a critical role in immunological functions including leukocyte recruitment and T-cell costimulation.¹

LFA-1 is expressed in a low affinity state on unactivated cells and switches to a high affinity state following cell activation.² LFA-1 is composed of two subunits, an α_L -subunit and a β_2 -subunit. The α_L -subunit contains a seven-bladed propeller region in which there is a 200 amino acid inserted domain at the N-terminus referred to as the I-Domain.² The I-Domain

consists of a central β -sheet surrounded by α -helices and two noninteracting binding sites. The MIDAS or metal-ion-dependent adhesion site is the site that directly interacts with ICAM. On the opposing end of the I-Domain is the IDAS or I-Domain allosteric site that indirectly affects the conformation of the MIDAS site to regulate the affinity of LFA-1. Specifically, a change in the IDAS site, from a closed to an open conformation, results in high affinity LFA-1/ICAM-1 interactions.² The β_2 -subunit contains an I-like domain, which is believed to serve a regulatory role and does not participate directly with the binding of ICAM.²

In vivo studies with anti-LFA-1 antibodies or with LFA-1 deficient mice have demonstrated that LFA-1 plays a critical role in leukocyte extravasation in recruitment models.³ Additionally, preclinical and clinical data from the humanized anti-LFA-1 antibody efalizumab, which was approved by the FDA in 2003 for the treatment of moderate to severe psoriasis, has provided proof-of-concept for this target.⁴ As a consequence, the LFA-1/ICAM-1 interaction has emerged as an attractive target for the treatment of immunological disorders such as psoriasis, rheumatoid arthritis, and solid organ transplantation.^{3–5}

As a result of the strong preclinical and clinical validation, there has been an intense effort to identify orally active small molecules that induce a targeted disruption of the LFA-1/ICAM-1 interaction as potential therapeutic agents. In this effort, our group⁶ and others^{5,7} have disclosed several diverse chemical series of compounds. NMR and X-ray crystallographic studies have established that many of these series bind to the IDAS site (I-Domain allosteric site) of the I-Domain

[†]PDB ID code 3M6F.

*To whom correspondence should be addressed. Phone: 609-252-6778. Fax: 609-252-7410. E-mail: scott.watterson@bms.com.

^aAbbreviations: LFA-1, leukocyte function associated antigen-1; ICAM, intercellular adhesion molecules; IDAS, I-Domain allosteric site; HUVEC, human umbilical vein endothelial cells; MLR, mixed lymphocyte reaction; b.END3, mouse brain endothelial cell line; SFC, super critical fluid chromatography; hERG, human ether-a-go-go-related gene; BAL, bronchoalveolar lavage; OVA, ovalbumin; PBMC, human peripheral blood mononuclear cells; APC, antigen presenting cell.

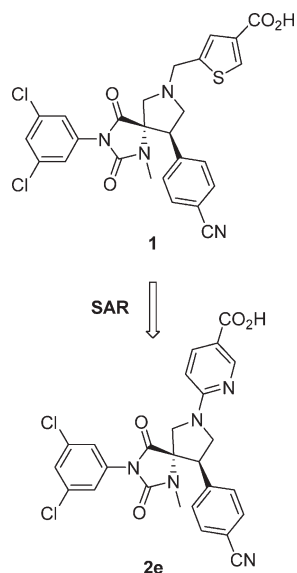


Figure 1

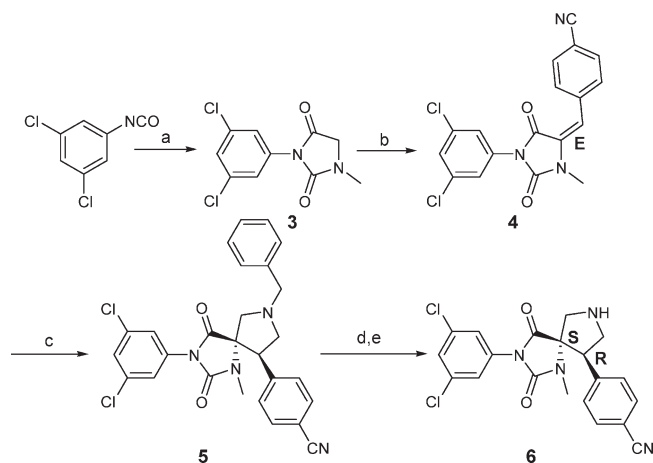
Table 1. In Vitro Potency of Spirocyclic Hydantoin Analogues^c

Cmpd	R	HUVEC ^a	MLR ^a
		IC ₅₀ (nM)	IC ₅₀ (nM)
1		18 ± 1.0	280 ± 20
2a		11 (n=2)	200 ± 70
2b		11 ^b	80 ± 20
2c		60 ^b	ND
2d		12 ± 1.0	140 ^b
2e		2.5 ± 0.4	60 ± 10

^a IC₅₀ values are shown as mean values of three determinations. ^b IC₅₀ values are shown as single determinations. ^c ND = not determined.

located on the α_L subunit.^{6–8} It has been reported that small molecule antagonists binding to the IDAS site prevent the conformational changes necessary for the conversion of the I-Domain from the low affinity, closed conformation to the high affinity, open conformation, consequently precluding the binding of ICAM.^{2a}

In an earlier report, we disclosed the structure–activity relationships (SAR) leading to a novel spirocyclic hydantoin antagonist (**1**, BMS-587101; Figure 1) of the LFA-1/ICAM-1 interaction.^{6b} Compound **1** inhibited LFA-1-mediated adhesion of human T-cells to human umbilical vein endothelial cells (HUVEC) and mouse T-cell adhesion to a mouse brain

Scheme 1^a

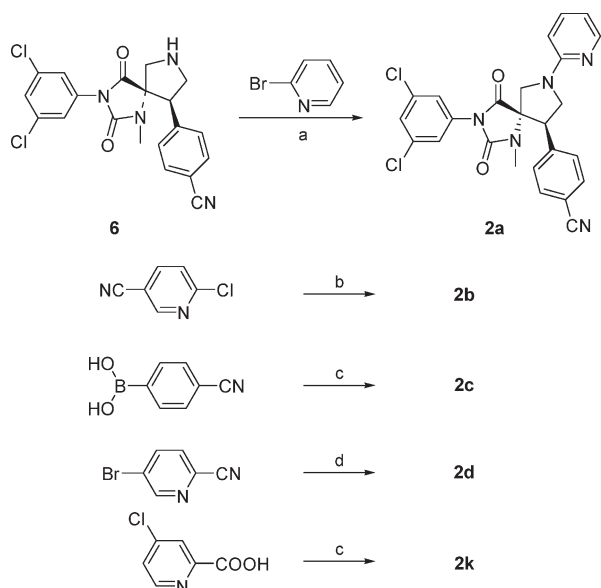
^a Reagents and conditions: (a) sarcosine ethyl ester, NaOH, THF/H₂O, 96%; (b) 4-cyanobenzaldehyde, β -alanine, AcOH, reflux, 35% or 4-cyanobenzaldehyde, pyrrolidine/EtOH, 78 °C 18 h, 85%; (c) *N*-(methoxymethyl)-*N*-(trimethylsilylmethyl)benzylamine, THF, TFA, 0 °C to RT, 18 h, 70%; (d) 1,2-dichloroethane, 1-chloroethyl chloroformate, 5 °C, to RT, 18 h, MeOH, reflux, 3 h, 50–85%; (e) Chiralpak-AD column, CO₂/MeOH, ~100% desired enantiomer (> 99% ee).

endothelial cell line (b.END3). It has been reported^{6b,9} that small molecule LFA-1 antagonists exhibit a significant disconnect with regard to inhibition of human LFA-1 vs rodent LFA-1, and to that end, **1** exhibited an approximately 8-fold decrease in potency. Additionally, in support of the role of LFA-1 in T-cell activation, **1** successfully blocked human T-cell proliferation in a mixed lymphocyte reaction (MLR) assay. Previously, we demonstrated that **1** was efficacious in combination with CTLA-4Ig in a mouse heart-to-ear transplant model.^{6b} Recently, we reported that **1** was able to robustly inhibit disease in two preclinical models of rheumatoid arthritis, a mouse antibody-induced arthritis (AIA) model and a mouse collagen-induced arthritis (CIA) model, even though **1** is ~8-fold less potent against mouse LFA-1.¹⁰ On the basis of its in vitro potency, in vivo activity, pharmacokinetic profile, and clean safety profile, compound **1** was advanced into the clinic.

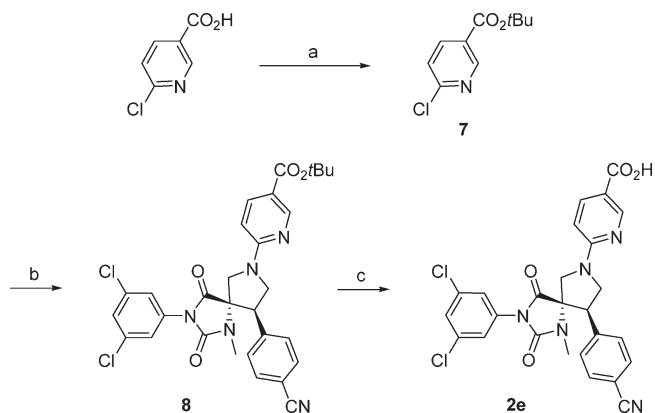
Having identified our first successful antagonist of LFA-1, we turned our attention to developing a next generation of spirocyclic hydantoin antagonists with enhanced potency. In this article, we outline the SAR leading to the identification of compound **2e** (BMS-688521;¹¹ Figure 1), which demonstrated significantly improved potency relative to compound **1**.

Chemistry

The synthetic pathways utilized in the preparation of the spirocyclic hydantoin antagonists discussed in Tables 1 and 4 are outlined in Schemes 1–9. The spirocyclic hydantoin core, 4-((5*S*,9*R*)-3-(3,5-dichlorophenyl)-1-methyl-2,4-dioxo-1,3,7-triazaspiro[4.4]nonan-9-yl)benzimidazole (**6**), was prepared as outlined in Scheme 1.^{6b,11} Knoevenagel condensation of **3** with 4-cyanobenzaldehyde gave the thermodynamically more stable benzylidene hydantoin **4**, which crystallized out of the reaction mixture as a single diastereomer having the desired *E* double bond stereochemistry. A subsequent azomethine ylide cycloaddition step with commercially available *N*-(methoxymethyl)-*N*-(trimethylsilylmethyl)benzylamine afforded compound **5** as a single diastereomer. *N*-Debenzylation utilizing modified Von Braun conditions afforded the des-benzyl analogue, which was

Scheme 2^a

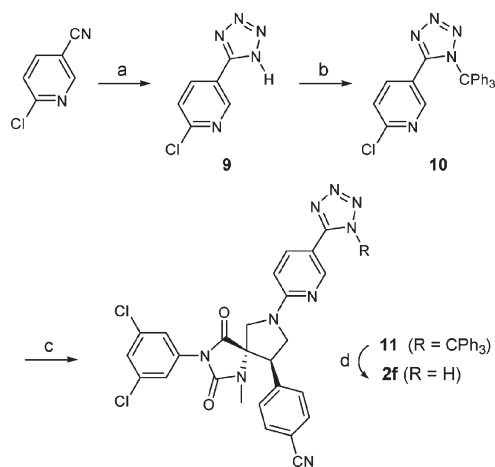
^a Reagents and conditions: (a) K_2CO_3 , DMF, 100 °C, 25%; (b) **6**, $\text{Pd}_2(\text{dba})_3$, biphenyl-2-ylidicyclohexylphosphine, *t*-BuOK, DMA, 85 °C, 41%; (c) **6**, $\text{Cu}(\text{OAc})_2$, Et_3N , CH_2Cl_2 , 100 °C, 14%; (d) **6**, $\text{Pd}_2(\text{dba})_3$, biphenyl-2-ylidicyclohexylphosphine, *t*-BuOK, DMA, 85 °C, 8%; (e) **6**, $\text{Pd}_2(\text{dba})_3$, BINAP, DIPEA, 90 °C, 33%.

Scheme 3^a

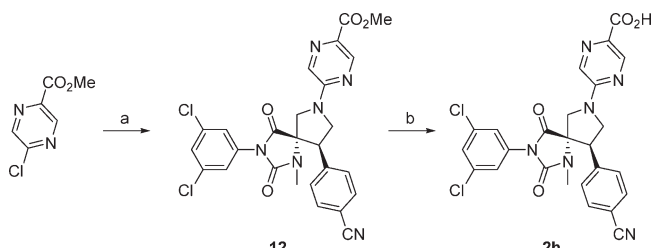
^a Reagents and conditions: (a) SOCl_2 ; *t*-BuOH, CH_2Cl_2 , Et_3N , DMAP, 70%; (b) **6**, DIPEA, DMA, 112 °C, 77%; (c) TFA, DCM, 86%.

separated into its individual enantiomers using a Chiralpak-AD column under supercritical fluid chromatography (SFC) conditions to give **6**. The intermediate **6** was determined to have >99% enantiomer excess, with the spirocyclic carbon assigned as (*S*) and the carbon bearing the 4-cyanophenyl residue assigned as (*R*), and was used as an intermediate for the preparation of all compounds discussed in this article.

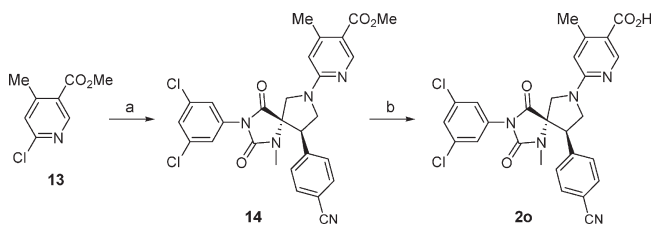
Analogues **2a–d** and **2k** were prepared as outlined in Scheme 2. Spirocyclic hydantoin **6** and 2-bromopyridine were heated at 100 °C in dimethylformamide in the presence of potassium carbonate to give **2a**. Analogues **2b**, **2d**, and **2k** were prepared via a Buchwald coupling¹² with either the appropriate bromo- or chloropyridine. A Chan–Lam coupling¹³ between 4-cyanoboronic acid and **6** afforded **2c**. Analogue **2e** was prepared as depicted in Scheme 3.¹¹ 6-Nicotinic acid was protected as a *tert*-butyl ester (**7**) in 70% yield. Heating of **7** with intermediate **6** at 112 °C in dimethylacetamide in the presence of diisopropylethylamine afforded *tert*-butyl ester **8**

Scheme 4^a

^a Reagents and conditions: (a) NaN_3 , Et_3N , AcOH, 130 °C, 30%; (b) Ph_3CCl , NaOH, CHCl_3 , 39%; (c) **6**, DIPEA, 118 °C, 12%; (d) TFA, MeOH.

Scheme 5^a

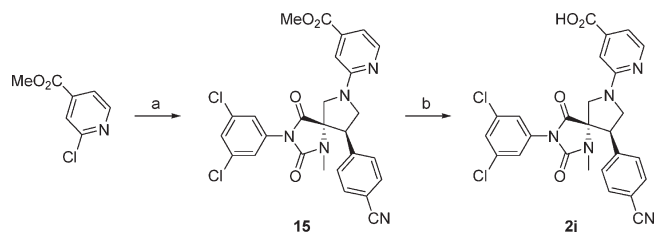
^a Reagents and conditions: (a) **6**, DIPEA, DMF, 100 °C, 86%; (b) 1 M aq KOH, 1,2-propanediol, THF, H_2O , 28%.

Scheme 6^a

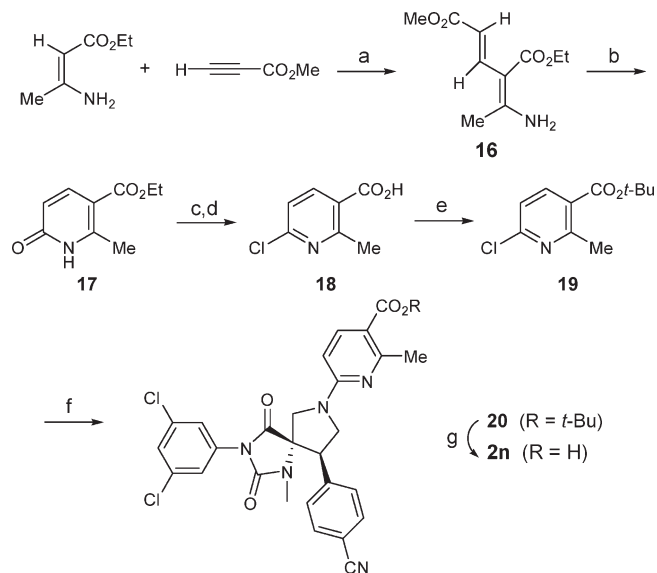
^a Reagents and conditions: (a) **6**, DIPEA, DMF, 100 °C, 81%; (b) LiI, DMA, 140 °C, 42%.

in 77% yield. The ester was subsequently hydrolyzed with trifluoroacetic acid to give **2e** in 86% yield. The carboxylic acid isostere, tetrazole **2f**, was prepared as outlined in Scheme 4.

Analogues **2g–i** and **2p–t** were prepared as outlined in Scheme 5 for the preparation of **2h**. Spirocyclic hydantoin intermediate **6** was heated in either dimethylformamide or dimethylacetamide with the appropriate chloro-, bromo-, or methylsulfone-substituted heteroaryl substrate, additionally substituted with a methyl or ethyl ester, at 95–110 °C to provide the intermediate esters in yields ranging from 28 to 97%. Subsequent hydrolysis of the ester with 1.0 M aqueous potassium hydroxide and 1,2-propanediol in a mixture of tetrahydrofuran and water afforded the desired analogues in yields ranging from 8 to 70%. The chloro-, bromo-, and methylsulfone-substituted heteroaryl substrates were commercially available, prepared as described in the literature, or synthesized as depicted in Scheme 9.

Scheme 7^a

^a Reagents and conditions: (a) **6**, neat, 96 °C, 37%; (b) LiI, DMA, 140 °C, 86%.

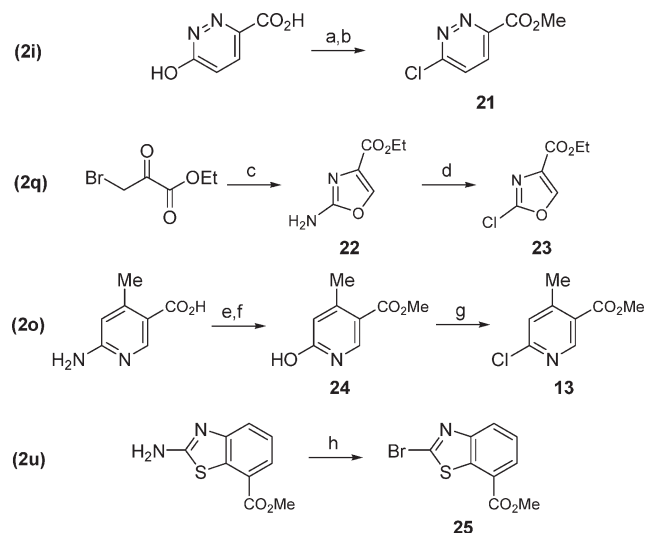
Scheme 8^a

^a Reagents and conditions: (a) neat, 108 °C, 72%; (b) DMF, reflux, 55%; (c) POCl₃, 128 °C; (d) NaOH (25% aq), 98%; (e) SOCl₂; *t*-BuOH, DMAP, Et₃N, 10% (f) **6**, DIPEA, DMA, 112 °C, 50%; (g) TFA, CH₂Cl₂, 76%.

Analogues **2o**, **2u**, and **2v** were prepared as shown in Scheme 6 for the preparation of **2o**. Spirocyclic hydantoin intermediate **6** was heated in either dimethylformamide or dimethylacetamide with the appropriate chloro-substituted heteroaryl substrate, additionally substituted with a methyl or ethyl ester, at 100–110 °C to provide the intermediate esters in yields ranging from 31 to 81%. Subsequent hydrolysis of the ester with either lithium iodide or lithium chloride in dimethylformamide, dimethylacetamide, or *N*-methyl-2-pyrrolidinone at 115–140 °C afforded the desired analogues in yields ranging from 39 to 86%. The chloro- and bromo-heteroaryl substrates were commercially available, prepared as described in the literature, or synthesized as depicted in Scheme 9.

Analogues **2j** was prepared as outlined in Scheme 7. Spirocyclic hydantoin intermediate **6** was heated neat with commercially available methyl 2-chloroisonicotinate at 96 °C to give the intermediate ester (**15**) in 37% yield. Subsequent hydrolysis of the ester with lithium iodide in dimethylacetamide at 140 °C afforded **2j** in 86% yield. Compound **2n** was prepared as depicted in Scheme 8.

Compounds outlined in Tables 1 and 4 were evaluated for LFA-1 mediated adhesion in a cell–cell based adhesion assay employing primary human T-cells and human umbilical vein endothelial cells (HUVEC) (see Experimental Section for details). Additionally, the activity of compounds on

Scheme 9^a

^a Reagents and conditions: (a) H₂SO₄, MeOH, reflux; (b) POCl₃; (c) urea, 100 °C, 40%; (d) *t*-BuONO, CuCl₂, MeCN, 65 °C, 66%; (e) SOCl₂, MeOH, 65%; (f) NaNO₂, H₂SO₄, H₂O, 71%; (g) POCl₃, 110 °C; (h) *t*-butyl nitrite, CuBr₂, MeCN.

APC-dependent T-cell proliferation was evaluated in vitro using a one-way mixed lymphocyte reaction (MLR) assay (see Experimental Section for details). In contrast to the adhesion assay, the MLR assay was conducted in the presence of 10% serum.

Results and Discussion

The X-ray co-crystal structure of spirocyclic hydantoin **1** with the I-Domain of LFA-1 (Figure 2) revealed that the compound binds to the I-Domain allosteric site (IDAS).^{6b} Additionally, the X-ray co-crystal structure revealed that most of the interactions of the ligand with the protein are hydrophobic in nature with the *p*-cyanophenyl aromatic ring forming a favorable edge-to-edge face π – π interaction with the *N*-3 3,5-dichlorophenyl ring in the pocket. The dichlorophenyl group itself occupies a hydrophobic pocket between α -helices 1 and 7 and β -strands 1, 3, and 4. The urea carbonyl is hydrogen-bonded to the amino acid residues Lys 287, Lys 305, and Glu 284 via a water molecule. Unlike the urea, the amide carbonyl does not appear to make any discernible contacts with the protein. As is evident from the crystal structure, the thiophene carboxylic acid moiety is projected into solvent and does not appear to interact with any residues in the I-Domain.

Since extensive SAR suggested that the 2,5-dichlorophenyl, *N*-methyl, and 4-cyanophenyl moieties are optimal,^{6b} we decided to focus on modulating potency, physicochemical properties, and liability profiling parameters with further modifications to the substitution on the spirocyclic pyrrolidine nitrogen. In particular, we reasoned based on the X-ray co-crystal structure that a heteroaryl group directly appended to the pyrrolidine nitrogen would engage in a hydrogen-bonding interaction with Tyr 257 (Figure 2) and improve potency compared to compound **1**. As seen in Table 1, our initial investigation into this hypothesis led to some promising results. The simple 1-pyridyl substituted derivative (**2a**) showed similar potency in both the T-cell/HUVEC adhesion assay (IC₅₀ = 11 nM) and the MLR T-cell proliferation assay (IC₅₀ = 200 nM) relative to our first

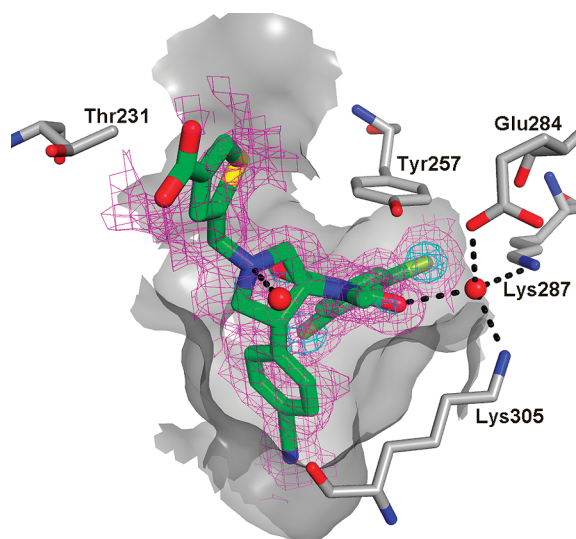


Figure 2. X-ray crystal structure of compound **1** bound to the I-Domain of LFA-1. Also shown is the initial electron density prior to fitting the compound (magenta $2F_o - F_c$ contoured at 1σ and cyan: $F_o - F_c$ contoured at 6σ , which indicates the positions of the chlorine atoms).

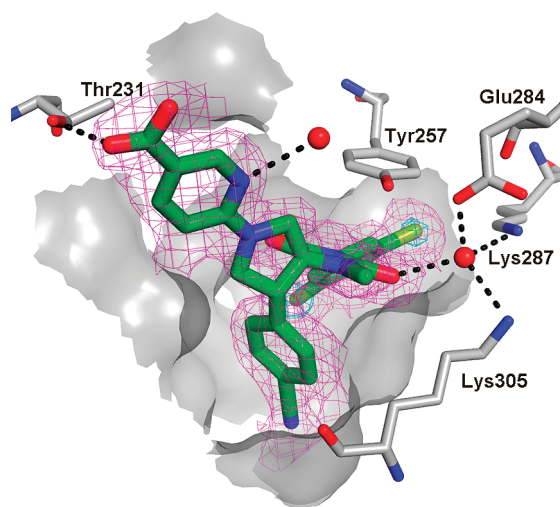


Figure 3. X-ray crystal structure of compound **2e** bound to the I-Domain of LFA-1. Also shown is the initial electron density prior to fitting the compound (magenta $2F_o - F_c$ contoured at 1σ and cyan: $F_o - F_c$ contoured at 6σ , which indicates the positions of the chlorine atoms).

clinical candidate (**1**). Addition of a 4-cyano substituent onto the pyridyl derivative (**2b**) maintained potency in the adhesion assay ($IC_{50} = 11$ nM) but resulted in a 3-fold increase in potency in the MLR assay. To understand the impact of the pyridyl nitrogen, the 4-cyanophenyl derivative was prepared (**2c**) and was found to be ~5-fold less potent than **2b** in the adhesion assay with an IC_{50} of 60 vs 11 nM, respectively, thus suggesting that the pyridyl nitrogen is likely involved in a hydrogen-bonding interaction with Tyr 257. To further explore the effects of the pyridyl nitrogen, the 4-cyano-3-pyridine derivative (**2d**) was prepared. As shown in Table 1, **2d** showed similar potency as **2b** with an IC_{50} of 12 nM in the adhesion assay and an IC_{50} of 140 nM in the MLR assay. This was surprising since one would expect that moving the pyridyl nitrogen adjacent to cyano group would not only affect the geometry of the hydrogen-bonding inter-

Table 2. Partial In Vitro Profiling Data for Compound **2e**^a

parameter	result
protein binding	95% in human serum
mutagenicity	Ames negative
hERG (patch clamp)	20% inhibition @ 30 μ M
Purkinje fiber	< 5% @ 30 μ M
CYP ^a inhibition (IC_{50})	> 35 μ M 1A2, 2C9, 2D6, 2C19, 3A4
Caco2 permeability (apical to basolateral)	148 nm/s

^aCYP = cytochrome P450.

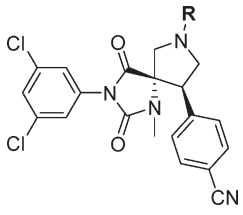
Table 3. Partial In Vitro Selectivity Data for Compound **2e**

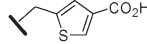
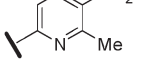
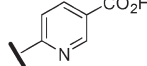
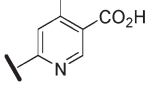
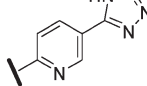
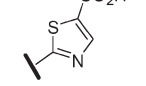
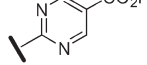
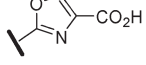
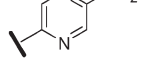
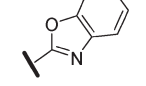
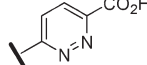
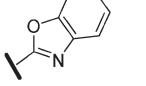
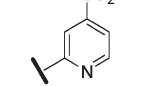
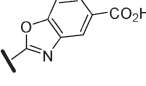
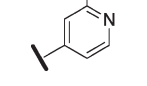
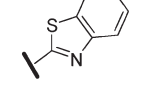
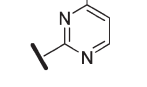
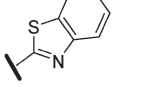
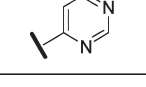
assay	selectivity	inhibition
THP-1 adhesion to i3Cb	Mac-1	18% @ 10 μ M
Jurkat: CS-1 adhesion	VLA-4	0% @ 10 μ M
platelet aggregation	$\alpha_2\beta_3$	
adenosine diphosphate		0% @ 30 μ M
collagen		0% @ 30 μ M

action but would also result in a more electron deficient nitrogen atom relative to the 2-pyridyl derivative, resulting in a less favorable hydrogen-bonding interaction.

Although compound **2b** was very promising, it was sub-optimal with respect to liability profiling and physicochemical properties. As we have found in our previous SAR around the pyrrolidine based spirocyclic hydantoin class,^{6b} incorporation of a carboxylic acid or carboxylic acid isostere resulted in zwitterionic compounds with optimal physicochemical properties and acceptable liability profiles (e.g., CYP inhibition, hERG, metabolic stability). Interestingly, the 4-carboxylic acid substituted 2-pyridine derivative (**2e**) was prepared and was found to be a highly potent inhibitor of the LFA-1/ICAM interaction with an IC_{50} of 2.5 nM in the adhesion assay and an IC_{50} of 60 nM in the MLR assay. This represented a 4–8-fold improvement in in vitro potency when compared to the initial program lead, **1**.

The X-ray co-crystal structure of **2e** bound to the I-Domain of LFA-1 (Figure 3) revealed that the carboxylic acid moiety is involved in a hydrogen-bonding interaction with the Thr 231 residue in the active site. The X-ray co-crystal structure also revealed that the pyridyl nitrogen is engaged in a hydrogen-bonding interaction with a water molecule that is in proximity to the Tyr 257 residue, although the distance between the water molecule and the residue was measured to be 3.7 Å in this crystal form, which is somewhat long for a typical hydrogen-bond length of 3.3 Å. All other interactions seen in the X-ray co-crystal structure of **1** are conserved. The ~5-fold loss in potency observed with the 4-cyanophenyl (**2c**) versus the 4-cyano-2-pyridyl (**2b**) would suggest that in a fully functioning protein, in an in vitro setting, the pyridyl nitrogen is potentially engaging in a hydrogen-bonding interaction with Tyr 257. Further analysis of the co-crystal structure of **2e** with molecular modeling suggests that a very small movement of either the water molecule or Tyr 257 does result in a hydrogen-bonding interaction with the pyridyl nitrogen. In considering the surprising activity seen with the 4-cyano-3-pyridyl analogue **2d**, a search of the Protein Data Bank (PDB) revealed that there are a number of examples of a pyridyl C–H α to the nitrogen interacting with a water molecule. It appears that the acidity of that hydrogen is sufficient enough to allow for an effective hydrogen-bond relative to the 4-cyanophenyl derivative (**2c**). Interestingly, by reducing the distance between the amino and the acid portions of the zwitterion, we have been able with **2e** to uncover a significant binding opportunity with

Table 4. In Vitro Potency of Spirocyclic Hytantonin Analogues^a


Cmpd	R	HUVEC ^a IC ₅₀ (nM)	MLR ^a IC ₅₀ (nM)	Cmpd	R	HUVEC ^a IC ₅₀ (nM)	MLR ^a IC ₅₀ (nM)
1		20 ± 1.0	280 ± 20	2n		12 ± 3.0	320 ± 60
2e		2.5 ± 0.4	60 ± 10	2o		11 ± 0.4	240 ± 90
2f		1.8 ± 0.6	80 ± 10	2p		5.0 ± 1.0	170 ± 30
2g		11 ± 3.0	260 ± 50	2q		58 (n=2)	ND
2h		19 ± 2.0	1260 ± 340	2r		4.8 ± 1.0	70 ± 20
2i		13 ± 5.0	270 ± 30	2s		6.0 ± 1.0	410 ± 50
2j		3.6 ± 1.7	50 ± 10	2t		4.0 ± 2.0	400 ± 70
2k		56	140 ± 60	2u		1.8 ± 0.3	80 ± 20
2l		26 ± 4.0	310 ± 50	2v		4.4 ± 1.4	280 ± 50
2m		8.0 ± 2.0	100 ± 20				

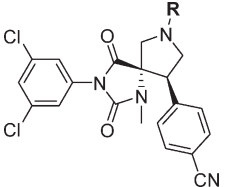
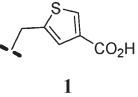
^a IC₅₀ values are shown as mean values of at least three determinations. ND = not determined.

the potential for a second, thus accounting for the observed increase in in vitro potency.

As expected, **2e** had a clean liability profile, as outlined in Table 2, as well as acceptable selectivity relative to other related integrins (Table 3). On the basis of the new X-ray crystallographic data, excellent in vitro potency, and a clean partial profile for **2e**, we turned our attention to further exploring and optimizing these interactions, as outlined in Table 4. As expected, the tetrazole carboxylic isostere (**2f**) was equipotent. Structural modeling based on the X-ray co-crystal structure suggested that moving the carboxylic acid to the

adjacent carbon would be tolerated and would still engage Thr 231. As predicted, moving the carboxylic acid to the 5-position of the pyridine ring (**2j**) demonstrated equipotent activity relative to **2e**. However, when the nitrogen was moved to the 4-position (**2k**), a loss in potency was observed. Compounds **2n** and **2o** represent an effort to structurally constrain the position of the pyridyl nitrogen and the carboxylic acid and to explore regions of the binding pocket. We rationalized that a small group adjacent to the carboxylic acid residue in **2e** might provide enhancements to the in vitro potency through restricted rotation of the carbonyl of the carboxylic acid, thus

Table 5. Comparison of **2e** and **1** (BMS-587101) in a Human IL-2 Whole Blood ex Vivo Assay

Cmpd		
HUVEC ^a (IC ₅₀ nM)	2.5 ± 0.4	20 ± 1.0
MLR ^a (IC ₅₀ nM)	63 ± 9.0	280 ± 20
bEND ^a (IC ₅₀ nM)	78 ± 16	150 ± 15
Human IL-2 ^a mRNA (IC ₅₀ nM)	65 ± 35	276 ± 34

^a IC₅₀ values are shown as mean values of at least three determinations.

optimizing the Thr 231 interaction. Interestingly, both derivatives were ~4 fold less potent than **2e**.

Other carboxylic acid substituted six-membered heterocycles were explored including pyrimidines (**2g**, **2l**, **2m**), a pyrazine (**2h**), and a pyridazine (**2i**), as seen in Table 4. With the exception of compound **2m**, incorporation of a second nitrogen into the six-membered heterocycle (**2l**, **2g–i**) led to a > 4-fold decrease in activity in the adhesion assay. On the basis of modeling studies, we had anticipated that the second nitrogen in the pyrimidine analogue (**2g**) might engage in an interaction with another Tyr residue (Tyr 166). Five-membered heterocycles were also explored. Thiazole **2p** was found to be a highly potent antagonist in both the adhesion and MLR assays (5.0 and 170 nM, respectively), although less optimized than **2e**. The oxazole derivative **2q** was substantially less potent than **2p**, with an IC₅₀ of 58 nM in the cell adhesion assay.

In continuing to leverage the X-ray co-crystal data from **2e**, we began to reason that carboxylic acid substituted bicyclic heterocycles would also be effective in engaging the Thr 231 interaction. With the support of molecular modeling, bicycles **2r–v** were prepared and evaluated, as seen in Table 4. As predicted, the 7-carboxylic acid benzoxazole **2r** and the 7-carboxylic benzothiazole **2u** demonstrated similar activity to that of lead **2e** in the adhesion and the MLR assays. As exemplified by compounds **2s**, **2t**, and **2v**, relocating the acid residue to either the 5- or 6-position of the bicycle maintained potency in the adhesion assay, although a 4- to 7-fold decrease in activity in the MLR assay was observed.

Although we prepared several highly potent antagonists of the LFA-1/ICAM-1 interaction, spirocyclic hydantoin **2e** demonstrated optimal in vitro potency with a desirable in vitro liability profile and was selected as our lead candidate. Compound **2e** was compared with **1** in a human IL-2 whole blood ex vivo assay where the level of IL-2 mRNA is assessed (Table 5). This assay was conducted on heparinized human whole blood that had been activated with SEB. This response can be blocked with anti-LFA-1 antibody, demonstrating that IL-2 production is LFA-1 dependent. IL-2 mRNA levels were determined based on the RNA isolated from activated cells at 6 h post stimulation. In this ex vivo assay, **2e** was found to be 4-fold more potent than **1** (IC₅₀ of 65 vs 276 nM; Table 5), which is consistent with the MLR data.

As previously mentioned, small molecule LFA-1 antagonists exhibit a significant disconnect with regard to the

Table 6. Pharmacokinetic Parameters for Compound **2e**^a

parameter	mouse	rat ^a	dog ^a
po dose (mg/kg)	5 ^b	5 ^b	5 ^b
iv dose (mg/kg)	1	1	1
C _{max} (μM), PO	0.32	2.3 ± 1.4	22 ± 4.9
T _{max} (μM), PO	1.0	1.7 ± 0.60	2.9 ± 2.0
AUC (μM·h), PO	1.5	13 ± 8.1	102 ± 32
T _{1/2} (h), iv	1.6	3.3 ± 0.80	4.7 ± 0.70
MRT (h), iv	1.7	3.5 ± 0.90	6.9 ± 0.80
Cl (mL/min/kg), iv	50	11 ± 5.6	0.50 ± 0.10
V _{ss} (L/kg), iv	5.1	2.3 ± 1.1	0.20 ± 0.10
F _{po} (%)	50	82	48

^a Average of three animals with associated standard deviation. ^b Vehicle: PEG400/0.1 M phosphate buffer (80/20 v/v).

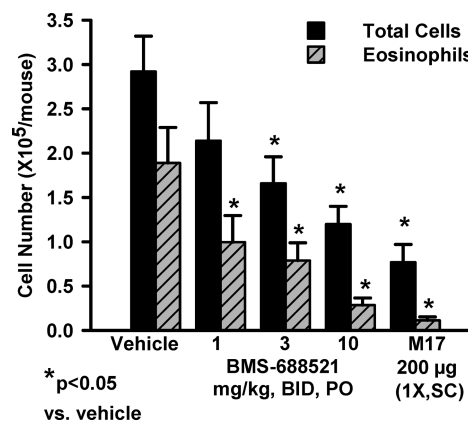


Figure 4. Efficacy of **2e** (1, 3, and 10 mg/kg) vs vehicle in a mouse allergic eosinophilic lung inflammation model. Mice ($n = 8$ /group) were immunized with OVA IP on day 0, boosted on day 14, and challenged on day 28; **2e** was administered PO/BID for 3 days starting on day 28. Vehicle: PEG400/0.1 M phosphate buffer (80/20 v/v). M17 is an anti-LFA-1 monoclonal antibody. * p value < 0.05 compared to vehicle treatment group.

inhibition of human LFA-1 vs rodent LFA-1. As a result of this cross species disconnect, we evaluated **2e** in a mouse-specific adhesion assay that employed mouse splenocytes and a mouse ICAM-1 expression cell line, b.END3. The original clinical candidate, **1**, was found to show activity in this assay with an IC₅₀ of 150 nM. This represents a 7- to 9-fold decrease in activity when compared to the results of the human T-cell/HUVEC adhesion assay data (IC₅₀ = 20 nM). As seen in Table 5, **2e** was found to have an IC₅₀ of 78 nM, representing an approximately 30-fold decrease in activity relative to the human T-cell/HUVEC assay data (IC₅₀ = 2.5 nM).

On the basis of its exceptional in vitro potency and clean profile, spirocyclic hydantoin **2e** was evaluated in vivo. In pharmacokinetic (PK) studies in mice, rats, and dogs (Table 6), bioavailabilities were around 50% or higher and half-lives ranged from 1.6–4.7 h. On the basis of its excellent in vitro potency, reasonable mouse LFA-1 antagonist activity, and its acceptable mouse PK profile, spirocyclic hydantoin **2e** was evaluated in a mouse allergic eosinophilic lung inflammation model. The ability of **2e** to block eosinophil accumulation in the airways of the lung, as measured in bronchoalveolar lavage (BAL) fluid, was evaluated in ovalbumin (OVA)-sensitized and challenged BALB/c mice. Mice were given OVA intraperitoneally (IP) on day 0, boosted on day 14, and given an intranasal challenge with OVA on day 28. Compound **2e** was given at doses of 1, 3, and 10 mg/kg, PO, BID for a three-day

duration following OVA challenge. Lungs were then lavaged and the cells quantified. Significant inhibition ($p < 0.05$ versus vehicle) of eosinophil accumulation was seen at a dose of 1 mg/kg BID (Figure 4), with dose-dependent inhibition at 3 mg/kg and 10 mg/kg. These results with **2e** approximate those seen with **1^{6b}** and the antimouse LFA-1 antibody, M17.

Conclusion

In summary, a novel second generation series of spirocyclic hydantoin antagonists of LFA-1 have been identified. Through exploring carboxylic acid substituted heterocycles appended to the pyrrolidine ring of the spirocyclic hydantoin core, we have been able to uncover a new structural interaction with Thr 231 and a potential second interaction with Tyr 257, as determined by the X-ray co-crystal of **2e** with the I-Domain of LFA-1. SAR studies led to multiple highly potent antagonists of LFA-1. On the basis of in vitro and ex vivo potency, in vivo activity, and pharmacokinetic and safety profiles, 6-((5*S*,9*R*)-9-(4-cyanophenyl)-3-(3,5-dichlorophenyl)-1-methyl-2,4-dioxo-1,3,7-triazaspiro[4.4]nonan-7-yl)nicotinic acid (**2e**) was selected as a lead compound. With the additional binding interactions, compound **2e** was found to have an approximately 4- to 8-fold improvement in human in vitro potency, a 4-fold improvement in a human IL-2 whole blood ex vivo assay, and a 2-fold higher free fraction relative to **1**. Compound **2e** was efficacious at a dose of 1 mg/kg BID in a mouse allergic eosinophilic lung inflammation model. On the basis of its preclinical profile and potential for improved efficacy in humans over **1**, spirocyclic hydantoin **2e** was advanced into clinical trials.

Experimental Section

Proton magnetic resonance (^1H) spectra were recorded on either a Bruker Avance 400 or a JEOL Eclipse 500 spectrometer and are reported in ppm relative to the reference solvent of the sample in which they were run. HPLC and LCMS analyses were conducted using a Shimadzu SCL-10A liquid chromatograph and a SPD UV-vis detector at 220 or 254 nm with the MS detection performed with either a Micromass Platform LC spectrometer or a Waters Micromass ZQ spectrometer. Preparative reverse-phase HPLC purifications were performed using the following conditions: YMC S5 ODS 20 mm \times 100 mm column with a binary solvent system where solvent A = 10% methanol, 90% water, 0.1% trifluoroacetic acid and solvent B = 90% methanol, 10% water, and 0.1% trifluoroacetic acid, flow rate = 20 mL/min, linear gradient time = 10 min, start %B = 20, final %B = 100. Fractions containing the product were concentrated in vacuo to remove the methanol and neutralized with aqueous sodium bicarbonate. The pH was adjusted to \sim 4.5–5.0, and the aqueous layer was extracted with organic solvents. The organic layer was collected, dried over anhydrous sodium sulfate or magnesium sulfate, and concentrated under reduced pressure. All flash column chromatography was performed on EM Science silica gel 60 (particle size of 40–60 μm). All reagents were purchased from commercial sources and used without further purification unless otherwise noted. All reactions were performed under an inert atmosphere.

HPLC analyses were performed using the following conditions. All final compounds had an HPLC purity of \geq 95% unless specifically mentioned.

Method A. A linear gradient using 5% acetonitrile, 95% water, and 0.05% TFA (solvent A) and 95% acetonitrile, 5% water, and 0.05% TFA (solvent B); $t = 0$ min, 10% B; $t = 15$ min, 100% B (20 min.) was employed on a SunFire C18 3.5 μ 4.6 mm \times 150 mm column. Flow rate was 1.0 mL/min and

UV detection was set to 220/254 nm. The LC column was maintained at ambient temperature.

Method B. A linear gradient using 5% acetonitrile, 95% water, and 0.05% TFA (solvent A) and 95% acetonitrile, 5% water, and 0.05% TFA (solvent B); $t = 0$ min, 10% B; $t = 15$ min, 100% B (20 min.) was employed on a XBridge Ph 3.5 μ 4.6 mm \times 150 mm column. Flow rate was 1.0 mL/min and UV detection was set to 220/254 nm. The LC column was maintained at ambient temperature.

Method C. A linear gradient using water/TFA (100/0.05) (solvent A) and acetonitrile/TFA (100/0.05) (solvent B); $t = 0$ min, 10% B; $t = 35$ min, 95% B (40 min.) was employed on a Luna C18(2) 0.46 cm \times 15 cm, 3 μ column. Flow rate was 1.0 mL/min and UV detection was set to 220 nm. The LC column was maintained at ambient temperature.

Method D. A linear gradient using 10% methanol, 90% water, and 0.2% H_3PO_4 (solvent A) and 90% methanol, 10% water, and 0.2% H_3PO_4 (solvent B); $t = 0$ min, 0% B; $t = 4$ min, 100% B (5 min.) was employed on a Chromolith SpeedROD 4.6 mm \times 50 mm column. Flow rate was 4.0 mL/min and UV detection was set to 220 nm. The LC column was maintained at ambient temperature.

Method E. A linear gradient using 10% methanol, 90% water, and 0.2% H_3PO_4 (solvent A) and 90% methanol, 10% water, and 0.2% H_3PO_4 (solvent B); $t = 0$ min, 0% B; $t = 4$ min, 100% B (5 min) was employed on a YMC ODS 4.6 mm \times 50 mm column. Flow rate was 4.0 mL/min and UV detection was set to 220 or 254 nm. The LC column was maintained at ambient temperature.

Method F. A linear gradient using 10% methanol, 90% water, and 0.2% H_3PO_4 (solvent A) and 90% methanol, 10% water, and 0.2% H_3PO_4 (solvent B); $t = 0$ min, 0% B; $t = 8$ min, 100% B (11 min) was employed on a Zorbax Rapid Res 3.5 μ 4.6 mm \times 50 mm column. Flow rate was 2.5 mL/min and UV detection was set to 220 nm. The LC column was maintained at ambient temperature.

Method G. A linear gradient using 10% methanol, 90% water, and 0.1% TFA (solvent A) and 90% methanol, 10% water, and 0.1% TFA (solvent B); $t = 0$ min, 0% B; $t = 4$ min, 100% B (5 min) was employed on a Phenomenex Phenom-Prime 4.6 mm \times 50 mm column. Flow rate was 4.0 mL/min and UV detection was set to 220 or 254 nm. The LC column was maintained at ambient temperature.

4-((5*S*,9*R*)-3-(3,5-Dichlorophenyl)-1-methyl-2,4-dioxo-7-(pyridin-2-yl)-1,3,7-triazaspiro[4.4]nonan-9-yl)benzotrile (2a). A mixture of **6** (0.100 g, 0.240 mmol), potassium carbonate (0.037 mg, 0.270 mmol), and 2-bromopyridine (0.025 mL, 0.260 mmol) was heated at 100 $^\circ\text{C}$ in dimethylformamide (1.0 mL) for 20 h. After cooling to room temperature, the insoluble salts were removed and the filtrate was partitioned between water and ethyl acetate. The aqueous layer was extracted with ethyl acetate, and the combined organic layers were washed with brine, concentrated under reduced pressure, and purified by flash silica gel chromatography to yield **2a** (30 mg, 25%) as a white solid. HPLC purity 97.1%; $t_r = 10.86$ min (method A); 95.9%; $t_r = 12.30$ min (method B). LCMS (EI) m/z Calcd for $\text{C}_{25}\text{H}_{19}\text{Cl}_2\text{N}_5\text{O}_2$ [$\text{M} + \text{H}$] $^+$ 492.10. Found: 492.10. ^1H NMR (500 MHz, CDCl_3) δ 3.24 (s, 3H), 3.95–4.30 (m, 5H), 6.50 (m, 1H), 6.70 (m, 1H), 6.79 (m, 2H), 7.10 (m, 1H), 7.39 (m, 2H), 7.70 (m, 3H), and 8.22 (m, 1H).

6-((5*S*,9*R*)-9-(4-Cyanophenyl)-3-(3,5-dichlorophenyl)-1-methyl-2,4-dioxo-1,3,7-triazaspiro[4.4]nonan-7-yl)nicotinonitrile (2b). A mixture of **6** (0.083 g, 0.200 mmol), 6-chloro-nicotinonitrile (0.040 g, 0.290 mmol), tris(dibenzylideneacetone)dipalladium(0) (0.046 g, 0.050 mmol), biphenyl-2-ylidicyclohexylphosphine (17.5 mg, 0.050 mmol), potassium *t*-butoxide (0.042 g, 0.380 mmol), and dimethylformamide (3.0 mL) was flushed well with nitrogen. The mixture was stirred at 85 $^\circ\text{C}$ overnight and then purified by preparative HPLC to provide **2b** (0.042 g, 41%) as a yellow solid. HPLC purity 99.1%; $t_r = 15.97$ min (method A); 99.1%; $t_r = 15.28$ min (method B). LCMS (EI) m/z Calcd for

$C_{26}H_{18}C_{12}N_6O_2 [M + H]^+$ 517.09. Found: 517.12. 1H NMR (500 MHz, $CDCl_3$) δ 3.24 (s, 3H), 3.94–4.04 (m, 2H), 4.09–4.22 (m, 2H), 4.34 (t, $J = 11.0$ Hz, 1H), 6.51 (d, $J = 8.80$ Hz, 1H), 6.80 (s, 2H), 7.29 (s, 1H), 7.38 (2H, d, $J = 8.25$ Hz), 7.66–7.75 (m, 3H), and 8.48 (s, 1H).

4,4'-(5*S*,9*R*)-3-(3,5-Dichlorophenyl)-1-methyl-2,4-dioxo-1,3,7-triazaspiro[4.4]nonane-7,9-diyl)dibenzonitrile (2c). To a solution of **6** (0.100 g, 0.240 mmol) in dichloromethane (5.0 mL) were sequentially added 4-cyanophenylboronic acid (0.071 g, 0.480 mmol), copper(II) acetate (0.066 g, 0.360 mmol), triethylamine (0.067 mL, 0.480 mmol), and 4 Å molecular sieves (0.200 g) at room temperature. The reaction mixture was stirred for 20 h exposed to the atmosphere and then quenched by the addition of aqueous ammonia (2.0 mL). After stirring at room temperature for 10 min, the reaction mixture was concentrated. To the resulting residue was added 20 mL of dichloromethane, and the contents were filtered over a pad of celite. The filtrate was concentrated under reduced pressure and purified by flash silica gel chromatography to yield **2c** (0.018 g, 14%) as a solid. HPLC purity 99.2%; $t_r = 16.48$ min (method A); 97.7%; $t_r = 15.81$ min (method B). LCMS (EI) m/z Calcd for $C_{27}H_{19}C_{12}N_5O_2 [M + H]^+$ 516.10. Found: 516⁺. 1H NMR (500 MHz, $CDCl_3$) δ 3.27 (s, 3H), 3.80–3.85 (m, 1H), 3.89–3.94 (m, 1H), 3.98–4.05 (m, 2H), 4.21–4.29 (m, 1H), 6.66 (d, $J = 9.06$ Hz, 2H), 6.80 (d, $J = 1.76$ Hz, 2H), 7.30 (t, $J = 1.76$ Hz, 1H), 7.40 (d, $J = 8.31$ Hz, 2H), 7.57 (d, $J = 8.81$ Hz, 2H), and 7.71 (d, $J = 8.56$ Hz, 2H).

5-((5*S*,9*R*)-9-(4-Cyanophenyl)-3-(3,5-dichlorophenyl)-1-methyl-2,4-dioxo-1,3,7-triazaspiro[4.4]nonan-7-yl)picolinonitrile (2d). A mixture of **6** (0.021 g, 0.050 mmol), 5-bromopicolinonitrile (13.7 mg, 0.075 mmol), tris(dibenzylideneacetone)dipalladium(0) (11.4 mg, 0.013 mmol), biphenyl-2-ylidicyclohexylphosphine (4.4 mg, 0.013 mmol), and potassium *t*-butoxide (10.6 mg, 0.095 mmol) was flushed well with nitrogen. Dimethylformamide (4.0 mL) was added, and the reaction mixture was stirred at 96 °C overnight. The mixture was diluted with dichloromethane, filtered through a pad of celite, and the filtrate was washed with water (2×), concentrated under reduced pressure, and purified by flash silica gel chromatography to provide **2d** (2.0 mg, 7.7%) as white solid. HPLC purity 99%; $t_r = 6.61$ min (method F); 99%; $t_r = 3.23$ min (method E). LCMS (EI) m/z Calcd for $C_{26}H_{18}C_{12}N_6O_2 [M + H]^+$ 517.09. Found: 517.10. 1H NMR (500 MHz, $CDCl_3$) δ 3.27 (s, 3H), 3.49–4.32 (m, 5H), 6.79 (d, $J = 1.65$ Hz, 2H), 6.93 (m, 1H), 7.31 (s, 1H), 7.39 (d, $J = 8.5$ Hz, 2H), 7.59 (d, $J = 8.25$ Hz, 1H), 7.71 (d, $J = 8.25$ Hz, 2H), and 8.14 (d, $J = 2.75$ Hz, 1H).

6-((5*S*,9*R*)-9-(4-Cyanophenyl)-3-(3,5-dichlorophenyl)-1-methyl-2,4-dioxo-1,3,7-triazaspiro[4.4]nonan-7-yl)nicotinic Acid (2e). A mixture of 6-chloronicotinic acid (12.0 g, 76.0 mmol) and thionyl chloride (65.0 mL) was heated at reflux for 3.0 h. The excess thionyl chloride was removed under reduced pressure, and the residual liquid was diluted with dichloromethane (20.0 mL) and then added to a solution of *tert*-butyl alcohol (71.0 mL, 760 mmol) in dichloromethane (40.0 mL). To the mixture was added triethylamine (31.7 mL, 760 mmol) and *N,N*-dimethylpyridine (0.500 g, 4.00 mmol), and the reaction mixture was stirred overnight (14 h) at reflux under nitrogen. The solution was diluted with dichloromethane (200 mL), washed with a saturated aqueous solution of sodium bicarbonate (3 × 100 mL), washed with water (3 × 100 mL), and dried over anhydrous sodium sulfate. Concentration under reduced pressure provided *tert*-butyl 6-chloronicotinate (**7**, 11.4 g, 70%) as a yellow solid. HPLC purity 96%; $t_r = 3.18$ min (method E). LCMS (EI) m/z Calcd for $C_{10}H_{12}ClNO_2 [M + H]^+$ 213.06. Found: 214⁺.

To a mixture of **6** (14.5 g, 34.9 mmol) and *tert*-butyl 6-chloronicotinate (**7**, 8.0 g, 35.6 mmol) in dimethylacetamide (50.0 mL) was added diisopropylethylamine (11.3 g, 87.3 mmol). The reaction mixture was stirred at 112 °C for 18 h under nitrogen. After cooling, the mixture was added slowly to ice water (200 mL) with stirring. After 10 min, the resulting precipitate was collected by vacuum filtration and washed with water (3 × 20 mL). The

crude product was dried and purified by flash silica gel chromatography using a mixture of ethyl acetate and dichloromethane (5–10%) to give *tert*-butyl 6-((5*S*,9*R*)-9-(4-cyanophenyl)-3-(3,5-dichlorophenyl)-1-methyl-2,4-dioxo-1,3,7-triazaspiro[4.4]nonan-7-yl)nicotinate (**8**) as yellow solid (15.8 g, 77%). HPLC $t_r = 3.91$ min (method E). LCMS (EI) m/z Calcd for $C_{30}H_{27}C_{12}N_5O_4 [M + H]^+$ 591.14. Found: 592⁺. 1H NMR (500 MHz, $CDCl_3$) δ = 1.59 (s, 9H), 3.26 (s, 3H), 3.95–4.25 (m, 5H), 6.47 (d, $J = 9.0$ Hz, 1H), 6.81–6.82 (m, 2H), 7.29–7.30 (m, 1H), 7.40 (d, $J = 8.0$ Hz, 2H), 7.70 (d, $J = 8.0$ Hz, 2H), 8.08 (dd, $J = 9.0$ and 2.4 Hz, 1H), and 8.82 (d, $J = 2.4$ Hz, 1H).

To the solution of *tert*-butyl 6-((5*S*,9*R*)-9-(4-cyanophenyl)-3-(3,5-dichlorophenyl)-1-methyl-2,4-dioxo-1,3,7-triazaspiro[4.4]nonan-7-yl)nicotinate (**8**, 15.5 g, 26.2 mmol) in dichloromethane (50.0 mL) was added trifluoroacetic acid (50.0 mL) dropwise with stirring between 0 and 5 °C. After the addition was complete, the ice water bath was removed and the mixture was stirred at room temperature for 3.5 h. The solvent was then removed under reduced pressure, and the residue was diluted with dichloromethane (400 mL) and water (100 mL). After stirring for 10 min, the pH of the aqueous layer was adjusted to ~9 with a saturated aqueous solution of sodium bicarbonate. The mixture was stirred for 15 min, and the pH was rechecked to ensure basicity. The pH was then adjusted to ~4.5 with a 1N aqueous solution of hydrochloric acid. After stirring for 15 min, the organic layer was collected and the aqueous layer was extracted with dichloromethane (50 mL). The organic phases were combined, washed with brine (100 mL), and dried over anhydrous sodium sulfate. Concentration under reduced pressure gave the crude product as a solid, which was dissolved in chloroform (55 mL) and stirred gently overnight at room temperature. The mixture was stirred for 30 min in an ice bath, and the resulting precipitate was collected by vacuum filtration. The white crystals were washed with cold chloroform (2 × 5 mL) and dried under reduced pressure to give the product (11.5 g). A second crop (0.600 g) was obtained through partial concentration of the mother liquor to give a total of 12.1 g (86%) of 6-((5*S*,9*R*)-9-(4-cyanophenyl)-3-(3,5-dichlorophenyl)-1-methyl-2,4-dioxo-1,3,7-triazaspiro[4.4]nonan-7-yl)nicotinic acid (**2e**) as a white solid.

HPLC purity 99.8%; $t_r = 13.03$ min (method B); 99.8%; $t_r = 19.63$ min (method C). LCMS (EI) m/z Calcd for $C_{26}H_{19}C_{12}N_5O_4 [M + H]^+$ 536.09. Found: 536.23 and 538.22. Anal. Calcd for $C_{26}H_{19}C_{12}N_5O_4$; 0.48% H_2O : C 57.92, H 3.61, N 12.99, Cl 13.19. Found C 57.77, H 3.54, N 12.79, Cl 13.07. 1H NMR (500 MHz, DMSO- d_6) δ 3.20 (s, 3H), 4.01 (d, $J = 12.10$ Hz, 1H), 4.13–4.21 (m, $J = 10.17$, 10.17 Hz, 3H), 4.37 (t, $J = 9.62$ Hz, 1H), 6.69 (d, $J = 8.25$ Hz, 1H), 6.81 (s, 2H), 7.48 (d, $J = 8.80$ Hz, 2H), 7.64 (s, 1H), 7.89 (d, $J = 8.80$ Hz, 2H), 8.02 (dd, $J = 8.80$, 2.20 Hz, 1H), 8.69 (s, 1H), and 12.57 (s, 1H). Enantiomeric excess = 100% [Chiralcel OD-H, 0.46 cm × 25 cm, 5 μ m particle size; EtOH/TFA (100:0.1)].

4-((5*S*,9*R*)-7-(5-(1*H*-Tetrazol-5-yl)pyridin-2-yl)-3-(3,5-dichlorophenyl)-1-methyl-2,4-dioxo-1,3,7-triazaspiro[4.4]nonan-9-yl)benzonitrile (2f). To a solution of 6-chloronicotinonitrile (2.76 g, 20.0 mmol) in anisole (30 mL) at 60 °C was added sequentially triethylamine (5.00 g, 50.0 mmol), acetic acid (3.00 g, 50.0 mmol), and sodium azide (3.30 g, 36.0 mmol). The reaction mixture was heated at 130 °C for 1.2 h and then cooled to 90 °C. Water (30 mL) followed by anisole (10 mL) was added, and the mixture was stirred for 10 min. The mixture was extracted with ethyl acetate (3×), and the aqueous layer was acidified to a pH of 5 with 2N aqueous hydrochloric acid and extracted with dichloromethane (3×). The organic layer was collected, dried over anhydrous sodium sulfate, and concentrated under reduced pressure to give 2-chloro-5-(1*H*-tetrazol-5-yl)pyridine (**9**, 1.10 g, 30%). HPLC purity 74%; $t_r = 1.77$ min (method D). 1H NMR (500 MHz, $CDCl_3$) δ 7.39 (d, $J = 8.25$ Hz, 1H), 8.44 (dd, $J = 8.25$, 2.20 Hz, 1H), and 9.17 (d, $J = 2.20$ Hz, 1H).

To the solution of 2-chloro-5-(1*H*-tetrazol-5-yl)pyridine (**9**, 0.360 g, 2.00 mmol) in chloroform (20 mL) was added a 10%

aqueous solution of sodium hydroxide (10 mL) and TBAB (0.064 g, 0.200 mmol). After stirring for 5 min, a solution of trityl chloride (0.668 g, 2.40 mmol) in chloroform (5.0 mL) was added dropwise. The mixture was stirred at room temperature for 3 h. The organic phase was separated, washed with a 10% aqueous solution of sodium hydroxide, washed with water, dried over anhydrous sodium sulfate, and concentrated under reduced pressure. The crude product was recrystallized from ethyl acetate/hexane (1:10) to give 2-chloro-5-(1-trityl-1*H*-tetrazol-5-yl)pyridine (**10**, 330 mg, 39%). HPLC purity 78%; t_r = 4.29 min (method D). $^1\text{H NMR}$ (500 MHz, CDCl_3) δ 7.11–7.46 (m, 16H), 8.35 (dd, J = 8.52, 2.47 Hz, 1H), and 9.12 (d, J = 2.20 Hz, 1H).

The mixture of **6** (0.021 g, 0.050 mmol), 2-chloro-5-(1-trityl-1*H*-tetrazol-5-yl)pyridine (**10**, 0.021 g, 0.050 mmol), and diisopropylethylamine (100 μL) was stirred at 120 °C overnight. After cooling, the diisopropylamine was removed under reduced pressure, and the crude product mixture (**11**) was dissolved in methanol (3.0 mL). Trifluoroacetic acid (1.0 mL) was added, and the mixture was stirred for 1 h at room temperature. Concentration under reduced pressure followed by purification by preparative HPLC provided **2f** as a white solid (3.3 mg, 12%). HPLC purity 97.7%; t_r = 13.21 min (method A); 96.9%; t_r = 13.01 min (method B). LCMS (EI) m/z Calcd for $\text{C}_{26}\text{H}_{20}\text{Cl}_2\text{N}_6\text{O}_4$ [$\text{M} + \text{H}$] $^+$ 560.11. Found: 560.11. $^1\text{H NMR}$ (500 MHz, methanol- d_4) δ 3.28 (s, 3H), 4.09–4.19 (m, 2H), 4.24 (s, 1H), 4.31–4.40 (m, 2H), 6.83 (d, J = 2.20 Hz, 2H), 6.89 (d, J = 9.35 Hz, 1H), 7.42 (s, 1H), 7.55 (d, J = 8.25 Hz, 2H), 7.79 (d, J = 8.25 Hz, 2H), 8.21 (dd, J = 9.35, 2.20 Hz, 1H), and 8.79 (d, J = 2.20 Hz, 1H).

2-((5*S*,9*R*)-9-(4-Cyanophenyl)-3-(3,5-dichlorophenyl)-1-methyl-2,4-dioxo-1,3,7-triazaspiro[4.4]nonan-7-yl)pyrimidine-5-carboxylic Acid (2g**).** A mixture of **6** (0.100 g, 0.241 mmol), ethyl 2-chloropyrimidine-5-carboxylate 14 (0.068 g, 0.362 mmol), and diisopropyl ethylamine (0.084 mL, 0.482 mmol) in anhydrous dimethylformamide (3 mL) was heated at 100 °C for 2 h. Water was added, the solvent was removed under reduced pressure, and the residue was diluted with dichloromethane, washed with water, and dried over anhydrous sodium sulfate. Concentration under reduced pressure followed by purification by flash silica gel chromatography using a 1:1 mixture of ethyl acetate and dichloromethane afforded ethyl 2-((5*S*,9*R*)-9-(4-cyanophenyl)-3-(3,5-dichlorophenyl)-1-methyl-2,4-dioxo-1,3,7-triazaspiro[4.4]nonan-7-yl)pyrimidine-5-carboxylate (0.054 g, 40%) as a white solid. HPLC purity 99%; t_r = 3.84 min (method D). LCMS (EI) m/z Calcd for $\text{C}_{27}\text{H}_{22}\text{Cl}_2\text{N}_6\text{O}_4$ [$\text{M} + \text{H}$] $^+$ 565.12. Found: 565.16 and 567.16. $^1\text{H NMR}$ (500 MHz, CDCl_3) δ 1.38 (t, J = 6.87 Hz, 3H), 3.24 (s, 3H), 3.97 (t, J = 9.62 Hz, 1H), 4.06 (d, J = 12.65 Hz, 1H), 4.24 (d, J = 13.20 Hz, 1H), 4.37 (q, J = 7.15 Hz, 2H), 4.45 (d, J = 9.90 Hz, 2H), 6.79 (s, 2H), 7.29 (s, 1H), 7.38 (d, J = 7.70 Hz, 2H), 7.69 (d, J = 8.25 Hz, 2H), and 8.94 (s, 2H).

A mixture of ethyl 2-((5*S*,9*R*)-9-(4-cyanophenyl)-3-(3,5-dichlorophenyl)-1-methyl-2,4-dioxo-1,3,7-triazaspiro[4.4]nonan-7-yl)pyrimidine-5-carboxylate (0.017 g, 0.031 mmol) and 1,2-propanediol (0.005 mL, 0.061 mmol) in tetrahydrofuran (1.0 mL) and water (0.5 mL) was stirred for 15 min at room temperature. A 1.0 M aqueous solution of potassium hydroxide (0.076 mL, 0.077 mmol) was added, and the reaction mixture was stirred for 7 h. To the mixture was added water (0.5 mL) followed by acetic acid (0.042 mL), and the tetrahydrofuran was removed under reduced pressure. The aqueous residue was diluted with water and dichloromethane, and the aqueous pH was adjusted to ~6.0 with 1N aqueous hydrochloric acid. The organic layer was collected, dried over anhydrous sodium sulfate, and concentrated under reduced pressure. The residue was purified by preparative HPLC to give **2g** (0.006 g) as a white solid. HPLC purity 97.2%; t_r = 14.31 min (method A); 97.0%; t_r = 13.72 min (method B). LCMS (EI) m/z Calcd for $\text{C}_{25}\text{H}_{18}\text{Cl}_2\text{N}_6\text{O}_4$ [$\text{M} + \text{H}$] $^+$ 537.08. Found: 537.19 and 537.16. $^1\text{H NMR}$ (500 MHz, CDCl_3) δ 3.26 (s, 3H), 3.98 (t, J = 8.8 Hz, 1H), 4.09 (d, J = 13.0 Hz, 1H), 4.28 (d, J = 13.0 Hz, 1H), 4.47–4.49 (m, 2H),

6.80 (s, 2H), 7.30 (s, 1H), 7.39 (d, J = 7.5 Hz, 2H), 7.70 (d, J = 7.5 Hz, 2H), and 8.98–8.99 (m, 2H).

5-((5*S*,9*R*)-9-(4-Cyanophenyl)-3-(3,5-dichlorophenyl)-1-methyl-2,4-dioxo-1,3,7-triazaspiro[4.4]nonan-7-yl)pyrazine-2-carboxylic Acid (2h**).** A mixture of **6** (0.100 g, 0.241 mmol), methyl 5-chloropyrazine-2-carboxylate (0.046 g, 0.265 mmol), and diisopropylethylamine (0.084 mL, 0.482 mmol) in anhydrous dimethylformamide (3.0 mL) was heated at 100 °C overnight. The solvent was removed under reduced pressure, and the residue was dissolved in dichloromethane, washed with water, and dried over anhydrous sodium sulfate. Concentration under reduced pressure followed by purification by preparative HPLC afforded methyl 5-((5*S*,9*R*)-9-(4-cyanophenyl)-3-(3,5-dichlorophenyl)-1-methyl-2,4-dioxo-1,3,7-triazaspiro[4.4]nonan-7-yl)pyrazine-2-carboxylate (0.114 g, 86%) (**12**) as a white solid. HPLC purity > 99%; t_r = 3.27 min (method D). LCMS (EI) m/z Calcd for $\text{C}_{26}\text{H}_{20}\text{Cl}_2\text{N}_6\text{O}_4$ [$\text{M} + \text{H}$] $^+$ 551.10. Found: 551.17 and 553.16. $^1\text{H NMR}$ (500 MHz, CDCl_3) δ 3.26 (s, 3H), 3.98 (s, 3H), 4.00–4.06 (m, 2H), 4.17 (d, J = 12.65 Hz, 1H), 4.30 (t, 1H), 4.43 (t, J = 11.00 Hz, 1H), 6.80 (s, 2H), 7.30 (s, 1H), 7.40 (d, J = 8.25 Hz, 2H), 7.70 (d, J = 8.25 Hz, 2H), 8.05 (s, 1H), and 8.89 (s, 1H).

A mixture of methyl 5-((5*S*,9*R*)-9-(4-cyanophenyl)-3-(3,5-dichlorophenyl)-1-methyl-2,4-dioxo-1,3,7-triazaspiro[4.4]nonan-7-yl)pyrazine-2-carboxylate (**12**, 0.099 g, 0.180 mmol) and 1,2-propanediol (0.026 mL, 0.360 mmol) in tetrahydrofuran (1.0 mL) and water (0.5 mL) was stirred for 15 min at room temperature. A 1.0 M aqueous solution of potassium hydroxide (0.45 mL, 0.450 mmol) was added, and the reaction mixture was stirred for 20 h. The tetrahydrofuran was removed under reduced pressure, and the aqueous residue was extracted with dichloromethane. The organic layer was collected, dried over anhydrous sodium sulfate, and concentrated under reduced pressure. The residue was purified by preparative HPLC to give **2h** (0.027 g) as a white solid. HPLC purity 97.8%; t_r = 13.63 min (method A); 94.5%; t_r = 13.25 min (method B). LCMS (EI) m/z Calcd for $\text{C}_{25}\text{H}_{18}\text{Cl}_2\text{N}_6\text{O}_4$ [$\text{M} + \text{H}$] $^+$ 537.08. Found: 537.45 and 539.40. $^1\text{H NMR}$ (500 MHz, $\text{DMSO}-d_6$) δ 3.20 (s, 3H), 4.02–4.12 (m, J = 10.45 Hz, 1H), 4.15–4.32 (m, 3H), 4.34–4.45 (m, J = 9.90 Hz, 1H), 6.82 (s, 2H), 7.49 (d, J = 8.25 Hz, 2H), 7.64 (s, 1H), 7.90 (d, J = 8.25 Hz, 2H), 8.13 (s, 1H), and 8.72 (s, 1H).

6-((5*S*,9*R*)-3-(3,5-Dichlorophenyl)-1-methyl-2,4-dioxo-9-phenyl-1,3,7-triazaspiro[4.4]nonan-7-yl)pyridazine-3-carboxylic Acid (2i**).** To a suspension of 6-hydroxypyridazine-3-carboxylic acid (2.00 g, 14.3 mmol) in methanol (50 mL) was added concentrated sulfuric acid (1.5 mL). The mixture was heated at reflux for 4 h, cooled to room temperature, and concentrated under reduced pressure to give a solid. The solid was suspended in ice water (50 mL), filtered under reduced pressure, and washed with additional ice water (50 mL). The precipitate was air-dried to give methyl 6-hydroxypyridazine-3-carboxylate (2.00 g). LCMS (EI) m/z Calcd for $\text{C}_6\text{H}_6\text{N}_2\text{O}_3$ [$\text{M} + \text{H}$] $^+$ 155.05. Found: 155 $^+$. The compound was used in the next step without any further purification.

Methyl 6-hydroxypyridazine-3-carboxylate (0.200 g) was suspended in phosphorus oxychloride (2.0 mL) and heated at 110 °C for 4 h. The reaction mixture was cooled to room temperature, the excess phosphorus oxychloride was removed under reduced pressure, and the resulting slurry was treated with ice water (5 mL). The resulting precipitate was filtered, rinsed with ice water (10 mL), and air-dried to give methyl 6-chloropyridazine-3-carboxylate (**21**, 110 mg). LCMS (EI) m/z Calcd for $\text{C}_6\text{H}_5\text{ClN}_2\text{O}_2$ [$\text{M} + \text{H}$] $^+$ 173.01. Found: 172.90. $^1\text{H NMR}$ (400 MHz, CDCl_3) δ 4.07 (s, 3H), 7.67 (d, J = 8.81 Hz, 1H), and 8.15 (d, J = 8.81 Hz, 1H).

To a solution of **6** (0.082 g, 0.200 mmol) and methyl 6-chloropyridazine-3-carboxylate (**21**, 0.040 g) in dimethylformamide (1.5 mL) was added diisopropylethylamine (0.090 mL, 0.500 mmol). The reaction mixture was heated at 95 °C for 4 h, cooled to room temperature, and purified by preparative HPLC to give

methyl 6-((5*S*,9*R*)-9-(4-cyanophenyl)-3-(3,5-dichlorophenyl)-1-methyl-2,4-dioxo-1,3,7-triazaspiro[4.4]nonan-7-yl)pyridazine-3-carboxylate as a trifluoroacetic acid salt (95 mg, 71%). LCMS (EI) *m/z* Calcd for C₂₆H₂₀Cl₂N₆O₄ [M + H]⁺ 551.10. Found: 553⁺. ¹H NMR (400 MHz, CDCl₃) δ 3.25 (s, 3H), 4.00 (s, 3H), 4.08 (m, 1H), 4.16–4.26 (m, 2H), 4.31 (m, 1H), 4.45 (t, *J* = 10.83 Hz, 1H), 6.80 (d, *J* = 2.01 Hz, 2H), 6.97 (d, *J* = 9.57 Hz, 1H), 7.30 (t, *J* = 2.01 Hz, 1H), 7.39 (d, *J* = 8.06 Hz, 2H), 7.70 (d, *J* = 8.06 Hz, 2H), and 8.10 (d, *J* = 9.57 Hz, 1H).

To a solution the methyl 6-((5*S*,9*R*)-9-(4-cyanophenyl)-3-(3,5-dichlorophenyl)-1-methyl-2,4-dioxo-1,3,7-triazaspiro[4.4]nonan-7-yl)pyridazine-3-carboxylate, trifluoroacetic acid salt (0.055 g, 0.100 mmol) in tetrahydrofuran (2.5 mL) and methanol (0.5 mL) was added 1,2-propanediol (0.020 mL) followed by 1*N* aqueous solution of potassium hydroxide (0.250 mL, 0.250 mmol). The mixture was stirred at room temperature for 4 h, acidified with a 10% aqueous solution of acetic acid to a pH of 5–6, and extracted with dichloromethane. The combined organic layers were filtered through a plug of a 1:1 MgSO₄/celite mixture, concentrated under reduced pressure, and purified by preparative HPLC to give **2i** as a trifluoroacetic acid salt, (12 mg, 37%). HPLC purity 98%; *t_r* = 6.04 min (method F); 98%; *t_r* = 3.00 min (method E). LCMS (EI) *m/z* Calcd for C₂₅H₁₈Cl₂N₆O₄ [M + H]⁺ 537.08. Found: 537⁺ and 539⁺. ¹H NMR (400 MHz, CD₃OD) δ 3.28 (s, 3H), 4.15–4.48 (m, 5H), 6.84 (s, 2H), 7.32 (d, *J* = 9.06 Hz, 1H), 7.43 (s, 1H), 7.56 (d, *J* = 8.06 Hz, 2H), 7.78 (d, *J* = 8.06 Hz, 2H), and 8.13 (d, *J* = 9.32 Hz, 1H).

2-((5*S*,9*R*)-9-(4-Cyanophenyl)-3-(3,5-dichlorophenyl)-1-methyl-2,4-dioxo-1,3,7-triazaspiro[4.4]nonan-7-yl)isonicotinic Acid (2j**).** A mixture of **6** (5.00 g, 0.012 mol) and 2-chloroisonicotinic acid, methyl ester (16.5 g, 0.096 mol), in a sealed tube was heated at 96 °C for 4.5 days. By HPLC, the reaction was complete. After cooling, the reaction mixture was diluted with dichloromethane, washed with a saturated aqueous solution of sodium bicarbonate, and dried over anhydrous sodium sulfate. Concentration under reduced pressure followed by purification by flash silica gel chromatography afforded methyl 2-((5*S*,9*R*)-9-(4-cyanophenyl)-3-(3,5-dichlorophenyl)-1-methyl-2,4-dioxo-1,3,7-triazaspiro[4.4]nonan-7-yl)isonicotinate (**15**, 2.45 g, 37%) as an off-white solid. HPLC purity > 98%; *t_r* = 3.24 min (method D). LCMS (EI) *m/z* Calcd for C₂₇H₂₁Cl₂N₅O₄ [M + H]⁺ 550.10. Found: 550.29 and 552.28. ¹H NMR (500 MHz, CDCl₃) δ 3.24 (s, 3H), 3.93 (s, 3H), 3.97–4.05 (m, 2H), 4.08–4.12 (m, 1H), 4.19 (t, *J* = 8.80 Hz, 1H), 4.30–4.35 (m, 1H), 6.79 (s, 2H), 7.09 (s, 1H), 7.22 (d, *J* = 5.50 Hz, 1H), 7.27 (s, 1H), 7.39 (d, *J* = 8.25 Hz, 2H), 7.68 (d, *J* = 8.25 Hz, 2H), and 8.32 (d, *J* = 4.95 Hz, 1H).

A mixture of methyl 2-((5*S*,9*R*)-9-(4-cyanophenyl)-3-(3,5-dichlorophenyl)-1-methyl-2,4-dioxo-1,3,7-triazaspiro[4.4]nonan-7-yl)isonicotinate (**15**, 1.55 g, 2.82 mmol) and lithium iodide (11.6 g) in anhydrous dimethylacetamide (15 mL) was heated at 140 °C overnight. HPLC analysis indicated that there was ~20% starting material remaining. An additional 5.0 g of lithium iodide was added, and the mixture was heated overnight. The reaction was cooled to room temperature, and acetic acid (~4.0 mL) was added followed by water (20 mL). The pH was adjusted to 5.0 with a 1.0 M aqueous solution of sodium hydroxide. The solid was collected by vacuum filtration, washed with water, and dried well under reduced pressure to give the product (1.40 g) as a light-brown solid. The compound was further purified by flash silica gel chromatography to give **2j** (1.30 g) as a yellow solid. HPLC purity 99.0%; *t_r* = 11.89 min (method A); 99.4%; *t_r* = 12.36 min (method B). LCMS (EI) *m/z* Calcd for C₂₆H₁₉Cl₂N₅O₄ [M + H]⁺ 536.09. Found: 536.23 and 538.22. ¹H NMR (500 MHz, DMSO-*d*₆) δ 3.20 (s, 3H) 3.98 (d, *J* = 12.10 Hz, 1H), 4.05–4.16 (m, 3H), 4.35 (t, *J* = 9.62 Hz, 1H), 6.80 (s, 2H), 7.05 (s, 1H), 7.08 (d, *J* = 4.95 Hz, 1H), 7.48 (d, *J* = 8.25 Hz, 2H), 7.63 (s, 1H), 7.88 (d, *J* = 8.25 Hz, 2H), and 8.21 (d, *J* = 4.95 Hz, 1H).

4-((5*S*,9*R*)-9-(4-Cyanophenyl)-3-(3,5-dichlorophenyl)-1-methyl-2,4-dioxo-1,3,7-triazaspiro[4.4]nonan-7-yl)picolinic Acid (2k**).** A mixture of **6** (0.021 mg, 0.050 mmol), 4-chloropicolinic acid

(11.8 mg, 0.075 mmol), tris(dibenzylideneacetone)dipalladium(0) (0.014 g, 0.016 mmol), BINAP (0.010 g, 0.016 mmol), and diisopropylamine (0.020 mL) was flushed well with nitrogen. Dimethylacetamide (2.0 mL) was added, and the mixture was stirred at 90 °C overnight. The mixture was diluted with dichloromethane (50 mL), filtered through a pad of celite, and the filtrate was washed with water (2×), concentrated under reduced pressure, and purified by preparative HPLC to provide **2k** (9.0 mg, 33%) as a white solid. HPLC purity 99%; *t_r* = 5.62 min (method F); 99%; *t_r* = 2.81 min (method E). LCMS (EI) *m/z* Calcd for C₂₆H₁₉Cl₂N₅O₄ [M + H]⁺ 536.09. Found: 536.18. ¹H NMR (500 MHz, CD₃OD) δ 3.21 (s, 3H), 4.10–4.30 (m, 5H), and 6.75–8.05 (m, 10H).

2-((5*S*,9*R*)-9-(4-Cyanophenyl)-3-(3,5-dichlorophenyl)-1-methyl-2,4-dioxo-1,3,7-triazaspiro[4.4]nonan-7-yl)pyrimidine-4-carboxylic Acid (2l**).** To a solution of **6** (100 mg, 0.240 mmol) in dimethylformamide (1.0 mL) was added methyl 2-(methylsulfonyl)pyrimidine-4-carboxylate¹⁵ (0.052 g, 0.240 mmol). The reaction mixture was allowed to heat for 4 h at 100 °C. The reaction mixture was diluted with water, extracted with diethyl ether, and concentrated under reduced pressure. The resulting residue was purified by flash silica gel chromatography to give methyl 2-((5*S*,9*R*)-9-(4-cyanophenyl)-3-(3,5-dichlorophenyl)-1-methyl-2,4-dioxo-1,3,7-triazaspiro[4.4]nonan-7-yl)pyrimidine-4-carboxylate (0.037 g, 28%). HPLC *t_r* = 3.59 min (method G). LCMS (EI) *m/z* Calcd for C₂₆H₂₀Cl₂N₆O₄ [M + H]⁺ 551.10. Found: 551⁺. ¹H NMR (500 MHz, CDCl₃) δ 3.19 (s, 3H), 3.91 (s, 3H), 3.91 (m, 1H), 4.03 (m, 1H), 4.21 (m, 1H), 4.39 (m, 2H), 6.72 (d, *J* = 1.65 Hz, 2H), 7.23 (m, 1H), 7.24 (d, *J* = 4.95 Hz, 1H), 7.33 (d, *J* = 8.25 Hz, 2H), 7.62 (d, *J* = 8.25 Hz, 2H), and 8.54 (m, 1H).

To a solution of methyl 2-((5*S*,9*R*)-9-(4-cyanophenyl)-3-(3,5-dichlorophenyl)-1-methyl-2,4-dioxo-1,3,7-triazaspiro[4.4]nonan-7-yl)pyrimidine-4-carboxylate (0.033 g, 0.060 mmol) in tetrahydrofuran (2.8 mL) and water (1.4 mL) was added 1,2-propanediol (0.083 mL). The mixture was stirred at room temperature for 5 min, at which point a 1.0 M aqueous solution of potassium hydroxide (0.147 mL) was added. After stirring for 2 h, the reaction mixture was concentrated under reduced pressure, and the resulting residue was neutralized with an ion-exchange resin to give **2l** as a white solid (22.5 mg, 70%). HPLC purity 98.1%; *t_r* = 14.11 min (method A); 97.3%; *t_r* = 13.52 min (method B). LCMS (EI) *m/z* Calcd for C₂₅H₁₈Cl₂N₆O₄ [M + H]⁺ 537.08. Found: 537⁺. ¹H NMR (500 MHz, DMSO-*d*₆) δ 3.19 (s, 3H), 3.96 (d, *J* = 12.1 Hz, 1H), 4.19 (m, 3H), 4.34 (m, 1H), 6.78 (m, 2H), 7.05 (d, *J* = 5.0 Hz, 1H), 7.46 (d, *J* = 8.25 Hz, 2H), 7.62 (m, 1H), 7.86 (d, *J* = 8.25 Hz, 2H), and 8.50 (d, *J* = 5.0 Hz, 1H).

6-((5*S*,9*R*)-9-(4-Cyanophenyl)-3-(3,5-dichlorophenyl)-1-methyl-2,4-dioxo-1,3,7-triazaspiro[4.4]nonan-7-yl)pyrimidine-4-carboxylic Acid (2m**).** To a mixture of **6** (0.096 g, 0.231 mmol) and methyl 6-chloropyrimidine-4-carboxylate¹⁶ (0.042 g, 0.231 mmol) in dimethylformamide (1.5 mL) was added diisopropylamine (0.121 mL, 0.691 mmol). The reaction mixture was heated for 2 h at 100 °C. The mixture was diluted with water, extracted with diethyl ether, and the organic layer was collected and dried over anhydrous sodium sulfate to give methyl 6-((5*S*,9*R*)-9-(4-Cyanophenyl)-3-(3,5-dichlorophenyl)-1-methyl-2,4-dioxo-1,3,7-triazaspiro[4.4]nonan-7-yl)pyrimidine-4-carboxylate (96 mg, 76%). HPLC *t_r* = 3.12 min (method G). LCMS (EI) *m/z* Calcd for C₂₆H₂₀Cl₂N₆O₄ [M + H]⁺ 551.10. Found: 551⁺. ¹H NMR (500 MHz, CDCl₃) δ 3.26 (s, 3H), 3.60 (m, 1H), 3.83 (m, 1H), 4.01 (s, 3H), 4.09 (m, 2H), 4.40 (m, 1H), 6.79 (m, 2H), 7.24 (s, 1H), 7.29 (s, 1H), 7.38 (d, *J* = 8.25 Hz, 2H), 7.69 (d, *J* = 8.25 Hz, 2H), 8.77 (m, 1H).

To a solution of methyl 6-((5*S*,9*R*)-9-(4-cyanophenyl)-3-(3,5-dichlorophenyl)-1-methyl-2,4-dioxo-1,3,7-triazaspiro[4.4]nonan-7-yl)pyrimidine-4-carboxylate (0.096 g, 0.174 mmol) in tetrahydrofuran (8.4 mL) and water (4.2 mL) was added 1,2-propanediol (0.25 mL). The reaction mixture was stirred at room temperature for 15 min, and then a 1.0 M aqueous solution of potassium hydroxide (0.440 mL) was added. After stirring at room temperature for 16 h, the reaction mixture was concentrated

under reduced pressure, and the resulting residue was purified by preparative HPLC to give **2m** as a white solid (34.6 mg, 37%). HPLC purity 95.0%; $t_r = 11.35$ min (method A); 94.8%; $t_r = 11.52$ min (method B). LCMS (EI) m/z Calcd for $C_{25}H_{18}Cl_2N_6O_4$ $[M + H]^+$ 537.08. Found: 537⁺. 1H NMR (500 MHz, DMSO- d_6) δ 3.19 (s, 3H), 4.00–4.40 (m, 5H), 6.79 (d, $J = 1.65$ Hz, 2H), 7.00 (brs, 1H), 7.48 (d, $J = 8.0$ Hz, 2H), 7.63 (dd, $J = 1.65, 1.65$ Hz, 1H), 7.87 (d, $J = 8.0$ Hz, 2H), 8.52 (s, 1H).

6-((5S,9R)-9-(4-Cyanophenyl)-3-(3,5-dichlorophenyl)-1-methyl-2,4-dioxo-1,3,7-triazaspiro[4.4]nonan-7-yl)-2-methylnicotinic Acid (2n). A mixture of ethyl-3-amino crotonate (5.20 g, 40.0 mmol) and methyl propiolate (3.40 g, 40.0 mmol) was stirred at 108 °C for 3 h under nitrogen. After cooling, the resulting solid was recrystallized from methanol to give (2E,4Z)-5-ethyl 1-methyl 4-(1-aminoethylidene)pent-2-enedioate as yellow solid (**16**, 6.10 g, 72%). HPLC purity > 95%; $t_r = 2.58$ min (method D). LCMS (EI) m/z Calcd for $C_{10}H_{15}NO_4$ $[M + H]^+$ 214.11. Found: 214.45. 1H NMR (500 MHz, $CDCl_3$) δ 1.35 (t, $J = 7.12$ Hz, 3H), 2.26 (s, 3H), 3.72 (s, 3H), 4.25 (q, $J = 7.12$ Hz, 2H), 6.17 (d, $J = 15.26$ Hz, 1H), and 7.64 (d, $J = 15.77$ Hz, 1H).

A mixture of (2E,4Z)-5-ethyl 1-methyl 4-(1-aminoethylidene)pent-2-enedioate (**16**, 6.00 g, 28.2 mmol) in dimethylformamide (30 mL) was heated at reflux for 14 h. After cooling, the resulting solid was collected by vacuum filtration, washed with dimethylformamide (3 \times), washed with diethyl ether (3 \times), and dried to give ethyl 2-methyl-6-oxo-1,6-dihydropyridine-3-carboxylate (**17**) as an off-white solid (2.8 g, 55%). HPLC purity > 95%; $t_r = 1.95$ min (method D). LCMS (EI) m/z Calcd for $C_6H_{11}NO_3$ $[M + H]^+$ 182.08. Found: 182.42. 1H NMR (500 MHz, $CDCl_3$) δ 1.35 (t, $J = 7.38$ Hz, 3H), 2.72 (s, 3H), 4.30 (q, $J = 7.12$ Hz, 2H), 6.41 (d, $J = 9.66$ Hz, 1H), 8.03 (d, $J = 9.66$ Hz, 1H), and 12.66 (s, 1H).

A mixture of ethyl 2-methyl-6-oxo-1,6-dihydropyridine-3-carboxylate (**17**, 0.610 g, 3.40 mmol) and phosphorus oxychloride (15 mL) was heated at 128 °C for 4 h. After cooling, the mixture was added to 100 mL of ice water, and the pH was then adjusted to 9 with a saturated aqueous solution of sodium bicarbonate. The aqueous mixture was extracted with ethyl acetate (3 \times), washed with a saturated aqueous solution of sodium chloride (2 \times), and dried over anhydrous sodium sulfate. Concentration under reduced pressure provided ethyl 6-chloro-2-methylnicotinate (2.3 g, 77%) as white solid. HPLC purity 98%; $t_r = 2.84$ min (method D). LCMS (EI) m/z Calcd for $C_9H_{10}ClNO_2$ $[M + H]^+$ 200.05. Found: 200.39. 1H NMR (500 MHz, $CDCl_3$) δ 1.39 (t, $J = 7.15$ Hz, 3H), 2.81 (s, 3H), 4.37 (q, $J = 7.15$ Hz, 2H), 7.23 (d, $J = 8.25$ Hz, 1H), and 8.15 (d, $J = 8.25$ Hz, 1H).

To a solution of ethyl 6-chloro-2-methylnicotinate (2.30 g, 11.5 mmol) and methanol (5.0 mL) was added a 25% aqueous solution of sodium hydroxide (1.0 mL) dropwise. The mixture was stirred at room temperature for 2.5 h. The pH was adjusted to 5–6 with acetic acid, and the solution was concentrated under reduced pressure to give the crude 6-chloro-2-methylnicotinic acid (**18**, 2.50 g, 98%), which was used to next step without further purification. HPLC purity 99%; $t_r = 1.62$ min (method D). LCMS (EI) m/z Calcd for $C_7H_6ClNO_2$ $[M + H]^+$ 172.02. Found: 172.36. 1H NMR (500 MHz, CD_3OD) δ 2.63 (s, 3 H), 7.23 (d, $J = 8.14$ Hz, 1H), and 7.84 (d, $J = 8.14$ Hz, 1H).

A mixture of 6-chloro-2-methylnicotinic acid (**18**, 0.172 g, 1.00 mmol) and thionyl chloride (5.0 mL) was stirred at reflux for 3 h. The excess of thionyl chloride was removed under reduced pressure. To the residue was added *t*-butanol (5.0 mL), dimethylaminopyridine (200 mg, 1.63 mmol), and triethylamine (1.0 mL), and the reaction mixture was stirred at 70 °C overnight under nitrogen. After cooling, the mixture was diluted with dichloromethane (100 mL), washed with a saturated aqueous solution of sodium bicarbonate, and dried over magnesium sulfate. Concentration under reduced pressure followed by purification by flash silica gel chromatography afforded *tert*-butyl 6-chloro-2-methylnicotinate (**19**, 0.022 g, 10%). HPLC purity 57%; $t_r = 3.40$ min (method D). LCMS (EI) m/z Calcd for

$C_{11}H_{14}ClNO_2$ $[M + H]^+$ 228.08. Found: 228.42. 1H NMR (500 MHz, $CDCl_3$) δ 1.58 (s, 9H), 2.77 (s, 3H), 7.20 (s, 1H), and 8.05 (d, $J = 8.14$ Hz, 1H).

A mixture of **6** (0.042 g, 0.100 mmol), *tert*-butyl 6-chloro-2-methylnicotinate (**19**, 0.022 g, 0.100 mmol), diisopropylethylamine (0.1 mL), and demethylacetamide (2.0 mL) was stirred at 112 °C for 18 h. After cooling, the mixture was added slowly to ice water (10 mL) and extracted with dichloromethane (3 \times). The organic layer was collected, dried over anhydrous sodium sulfate, and concentrated under reduced pressure. The residue was purified by flash silica gel chromatography to provide *tert*-butyl 6-((5S,9R)-9-(4-cyanophenyl)-3-(3,5-dichlorophenyl)-1-methyl-2,4-dioxo-1,3,7-triazaspiro[4.4]nonan-7-yl)-2-methylnicotinate (**20**, 30 mg, 50%). HPLC purity 74%; $t_r = 3.98$ min (method D). LCMS (EI) m/z Calcd for $C_{31}H_{29}Cl_2N_5O_4$ $[M + H]^+$ 606.17. Found: 606.14. 1H NMR (500 MHz, $CDCl_3$) δ 1.56–1.60 (m, 9H), 2.70 (s, 3H), 3.23 (s, 3H), 3.94–4.04 (m, 2H), 4.16 (d, $J = 11.70$ Hz, 2H), 4.23–4.32 (m, 1H), 6.29–6.35 (m, 1H), 6.80 (d, $J = 2.03$ Hz, 2H), 7.26 (t, $J = 5.34$ Hz, 1H), 7.38 (d, $J = 8.14$ Hz, 2H), 7.61–7.70 (m, 2H), and 8.04 (d, $J = 8.65$ Hz, 1H).

To *tert*-butyl 6-((5S,9R)-9-(4-cyanophenyl)-3-(3,5-dichlorophenyl)-1-methyl-2,4-dioxo-1,3,7-triazaspiro[4.4]nonan-7-yl)-2-methylnicotinate (**20**, 0.030 g, 0.050 mmol) in dichloromethane (2.0 mL) was added trifluoromethane (2.0 mL) at 0 °C. The mixture was stirred at room temperature for 2.5 h. The solvent and excess trifluoromethane was removed under reduced pressure, and the residue was purified with preparative HPLC to give **2n** (0.021 g, 76%) as a white solid. HPLC purity 99%; $t_r = 6.42$ min (method F); 99%; $t_r = 2.58$ min (method D). LCMS (EI) m/z Calcd for $C_{27}H_{21}Cl_2N_5O_4$ $[M + H]^+$ 550.10. Found: 550.08. 1H NMR (500 MHz, $CDCl_3$) δ 2.77 (s, 3H), 3.25 (s, 3H), 3.99–4.14 (m, 3H), 4.21 (d, $J = 10.45$ Hz, 1H), 4.34 (d, $J = 11.00$ Hz, 1H), 6.39 (d, $J = 9.35$ Hz, 1H), 6.80 (s, 2H), 7.28 (s, 1H), 7.38 (d, $J = 8.25$ Hz, 2H), 7.67 (d, $J = 8.25$ Hz, 2H), and 8.18 (d, $J = 8.80$ Hz, 1H).

6-((5S,9R)-9-(4-Cyanophenyl)-3-(3,5-dichlorophenyl)-1-methyl-2,4-dioxo-1,3,7-triazaspiro[4.4]nonan-7-yl)-4-methylnicotinic Acid (2o). To a heterogeneous mixture of 6-amino-4-methylnicotinic acid (1.00 g, 6.50 mmol) in methanol (20 mL) was added dropwise thionyl chloride (0.90 mL, 8.20 mmol). The mixture was refluxed for 20 h, cooled to room temperature, and the solvent was removed under reduced pressure. The resulting solid was dissolved in water (25 mL), and the pH was adjusted to 13 with a 1N aqueous solution of sodium hydroxide to give a white solid. The solid was collected by vacuum filtration, rinsed with water (25 mL), and air-dried to give methyl 6-amino-4-methylnicotinate (700 mg, 65%). LCMS (EI) m/z Calcd for $C_8H_{10}N_2O_2$ $[M + H]^+$ 167.08. Found: 167⁺. 1H NMR (500 MHz, DMSO- d_6) δ 2.37 (s, 3H), 3.72 (s, 3H), 6.25 (s, 2H), 6.62 (s, 2H), and 8.45 (s, 1H).

To an ice cold 15% aqueous solution of sulfuric acid (30 mL) was added methyl 6-amino-4-methylnicotinate (1.40 g, 8.4 mmol) followed by portionwise addition of sodium nitrite (1.20 g, 16.8 mmol). The reaction mixture was stirred at 0 °C for 2 h and at room temperature for an additional 2 h. The resulting solid was collected by vacuum filtration, rinsed sequentially with water (35 mL) and diethyl ether (35 mL), and air-dried to give methyl 6-hydroxy-4-methylnicotinate (**24**, 1.00 g, 71%). LCMS (EI) m/z Calcd for $C_8H_9NO_3$ $[M + H]^+$ 168.07. Found: 168⁺. 1H NMR (400 MHz, DMSO- d_6) δ 2.37 (s, 3H), 3.72 (s, 3H), 6.25 (s, 1H), 6.62 (s, 2H), and 8.46 (s, 1H).

To a suspension of methyl 6-hydroxy-4-methylnicotinate (**24**, 0.250 g, 1.50 mmol) in toluene (5.0 mL) was added phosphorus oxychloride (1.0 mL). The mixture was heated at 110 °C for 4 h, cooled to room temperature, and the excess phosphorus oxychloride was removed under reduced pressure. The resulting slurry was diluted with dichloromethane (25 mL) and washed sequentially with a saturated aqueous solution of sodium bicarbonate and water. The organic layer was collected and dried over anhydrous sodium sulfate. The solvent was removed under reduced pressure to give methyl 6-chloro-4-methylnicotinate

(**13**, 0.200 g, 72%) as a solid. (EI) m/z Calcd for $C_8H_8ClNO_2$ $[M + H]^+$ 186.03. Found: 186⁺ and 188⁺. ¹H NMR (400 MHz, DMSO-*d*₆) δ 2.53 (s, 3H), 3.85 (s, 3H), 7.58 (s, 1H), and 8.74 (s, 1H).

To a solution of **6** (0.165 g, 0.400 mmol) in *N*-methylpyrrolidine (1.5 mL) was added methyl 6-((5*S*,9*R*)-9-(4-cyanophenyl)-3-(3,5-dichlorophenyl)-1-methyl-2,4-dioxo-1,3,7-triazaspiro[4.4]nonan-7-yl)-4-methylnicotinate (**13**, 0.075 g, 0.400 mmol) and diisopropylethylamine (0.175 mL, 1.00 mmol). The reaction mixture was heated at 100 °C for 18 h, cooled to room temperature, and diluted with water (20 mL). The resulting solid was collected by vacuum filtration, rinsed with additional water (25 mL), rinsed with heptane (25 mL), and air-dried to give methyl 6-((5*S*,9*R*)-9-(4-cyanophenyl)-3-(3,5-dichlorophenyl)-1-methyl-2,4-dioxo-1,3,7-triazaspiro[4.4]nonan-7-yl)-4-methylnicotinate (**14**, 0.185 g). LCMS (EI) m/z Calcd for $C_{28}H_{23}Cl_2N_5O_4$ $[M + H]^+$ 564.12. Found: 566⁺. ¹H NMR (400 MHz, CDCl₃) δ 2.72 (s, 3H), 3.24 (s, 3H), 3.91 (s, 3H), 4.04–4.15 (m, 2H), 4.21 (m, 1H), 4.35 (m, 1H), 4.48 (t, J = 11.0 Hz, 1H), 6.58 (s, 1H), 6.79 (d, J = 1.5 Hz, 2H), 7.30 (t, J = 1.5 Hz, 1H), 7.37 (d, J = 8.0 Hz, 2H), 7.72 (t, J = 8.0 Hz, 2H), and 8.77 (s, 1H).

Methyl 6-((5*S*,9*R*)-9-(4-cyanophenyl)-3-(3,5-dichlorophenyl)-1-methyl-2,4-dioxo-1,3,7-triazaspiro[4.4]nonan-7-yl)-4-methylnicotinate (**14**, 0.050 g, 0.089 mmol) and lithium iodide (0.025 g, 0.140 mmol) were suspended in *N*-methylpyrrolidine (1.0 mL) and heated at 140 °C for 20 h. The mixture was cooled to room temperature, diluted with methanol (3.0 mL), and purified by preparative HPLC to give the product as a trifluoroacetic acid salt. The trifluoroacetic acid salt was dissolved in methanol (1.0 mL) and neutralized on a CUBCX1-HL (benzenesulfonic acid) ion exchange cartridge (UCT part number CUBX1HL5R3, 500 mg) to afford **20** as a solid (0.020 g, 42%). HPLC purity 96.5%; t_r = 12.22 min (method A); 97.4%; t_r = 12.84 min (method B). LCMS (EI) m/z Calcd for $C_{27}H_{21}Cl_2N_5O_4$ $[M + H]^+$ 550.10. Found: 550⁺ and 552⁺. ¹H NMR (400 MHz, CDCl₃/CD₃OD) δ 2.49 (s, 3H), 3.15 (s, 3H), 3.89–4.01 (m, 3H), 4.07 (t, J = 7.73 Hz, 1H), 4.22 (t, J = 10.7 Hz, 1H), 6.24 (s, 1H), 6.69 (d, J = 1.53 Hz, 2H), 7.20 (t, J = 1.53 Hz, 1H), 7.32 (d, J = 8.14 Hz, 2H), 7.60 (d, J = 8.14 Hz, 2H), and 8.68 (s, 1H).

2-((5*S*,9*R*)-9-(4-Cyanophenyl)-3-(3,5-dichlorophenyl)-1-methyl-2,4-dioxo-1,3,7-triazaspiro[4.4]nonan-7-yl)thiazole-5-carboxylic Acid (2p**)**. A mixture of **6** (0.187 g, 0.450 mmol), methyl 2-bromothiazole-5-carboxylate (0.111 g, 0.500 mmol), and diisopropylamine (0.10 mL) in dimethylacetamide was stirred at 105 °C for 4.5 h. After cooling, the mixture was added dropwise to ice water (50 mL). The resulting precipitate was collected by vacuum filtration, washed with water (3 \times), and dried to give methyl 2-((5*S*,9*R*)-9-(4-cyanophenyl)-3-(3,5-dichlorophenyl)-1-methyl-2,4-dioxo-1,3,7-triazaspiro[4.4]nonan-7-yl)thiazole-5-carboxylate (0.215 g, 86%). HPLC purity > 95%; t_r = 3.60 min (method D). LCMS (EI) m/z Calcd for $C_{25}H_{19}Cl_2N_5O_4S$ $[M + H]^+$ 556.06. Found: 556.08. ¹H NMR (500 MHz, CDCl₃) δ 3.25 (s, 3H), 3.83 (s, 3H), 4.06–4.15 (m, 3H), 4.33–4.41 (m, 2H), 6.82 (d, J = 2.03 Hz, 2H), 7.43 (s, 1H), 7.52 (d, J = 8.65 Hz, 2H), 7.78 (d, J = 8.14 Hz, 2H), and 7.93 (s, 1H).

To a mixture of methyl 2-((5*S*,9*R*)-9-(4-cyanophenyl)-3-(3,5-dichlorophenyl)-1-methyl-2,4-dioxo-1,3,7-triazaspiro[4.4]nonan-7-yl)thiazole-5-carboxylate (0.040 mg, 0.072 mmol) in tetrahydrofuran (2.0 mL) and water (1.0 mL) was added 1,2-propanediol (0.011 g, 0.144 mmol) followed by a 1*N* aqueous solution of potassium hydroxide (0.180 mL, 0.180 mmol). The mixture was stirred at room temperature overnight. After adjusting the pH to 4–5, the mixture was concentrated under reduced pressure. The residue was diluted with water (20 mL) and extracted with dichloromethane (3 \times). The organic layer was washed with water, dried over anhydrous sodium sulfate, and concentrated under reduced pressure. The residue was purified by preparative HPLC to give (**2p**, 16.0 mg, 41%) as white solid (41%). HPLC purity 98.9%; t_r = 14.57 min (method A); 97.8%; t_r = 13.96 min (method B). LCMS (EI) m/z Calcd for $C_{24}H_{17}Cl_2N_5O_4S$ $[M + H]^+$ 542.05. Found: 542.18. ¹H NMR (500 MHz, CD₃OD) δ 3.25 (s, 3H), 4.08 (m, 3H), 4.37 (m, 2H), 6.82 (d, J = 1.65 Hz, 2H), 7.42 (s, 1H), 7.52 (d, J = 8.25 Hz, 2H), 7.78 (d, J = 8.25 Hz, 2H), and 7.88 (s, 1H).

2-((5*S*,9*R*)-9-(4-Cyanophenyl)-3-(3,5-dichlorophenyl)-1-methyl-2,4-dioxo-1,3,7-triazaspiro[4.4]nonan-7-yl)oxazole-4-carboxylic Acid (2q**)**. A mixture of ethyl bromopyruvate (6.00 g, 0.030 mol) and urea (3.00 g, 0.050 mol) was heated at 100 °C for 1 h under nitrogen. To the brown solid was added water (50 mL), and the pH was adjusted to ~9–10 with a 1*N* aqueous solution of potassium hydroxide. The mixture was extracted with diethyl ether (3 \times), and the organic layer was washed with water (2 \times), dried over anhydrous sodium sulfate, and concentrated under reduced pressure to provide ethyl 2-aminooxazole-4-carboxylate (**22**, 1.87 g, 40%) as a yellow solid. HPLC purity 78%; t_r = 0.830 min (method D). LCMS (EI) m/z Calcd for $C_6H_8N_2O_3$ $[M + H]^+$ 157.06. Found: 157.35. ¹H NMR (500 MHz, CDCl₃) δ 1.34 (t, J = 7.12 Hz, 3H), 4.32 (q, J = 7.12 Hz, 2H), 5.13 (s, 2H), and 7.72 (s, 1H).

To a mixture of *tert*-butyl nitrite (0.990 g, 9.60 mmol) and copper(II) chloride (1.29 g, 9.60 mmol) in anhydrous acetonitrile (5.0 mL) was added ethyl 2-aminooxazole-4-carboxylate (**22**, 1.00 g, 6.40 mmol) dissolved in acetonitrile (2.0 mL) at 65 °C. Once nitrogen evolution subsided (~20 min), the solution was cooled to room temperature and poured into 150 mL of a 20% aqueous solution of hydrochloric acid. The mixture was extracted with diethyl ether (3 \times), washed with a 20% aqueous solution of hydrochloric acid, dried over anhydrous sodium sulfate, and concentrated under reduced pressure to provide ethyl 2-chlorooxazole-4-carboxylate (**23**, 0.740 g, 66%) as yellow oil. HPLC purity 84%; t_r = 1.93 min (method D). LCMS (EI) m/z Calcd for $C_6H_6ClNO_3$ $[M + H]^+$ 176.01. Found: 176.36. ¹H NMR (500 MHz, CDCl₃) δ 1.37 (t, J = 7.12 Hz, 3H), 4.38 (q, J = 7.12 Hz, 2H), and 8.18 (s, 1H).

The mixture of **6** (0.200 g, 0.480 mmol), ethyl 2-chlorooxazole-4-carboxylate (**23**, 0.120 g, 0.680 mmol), diisopropylamine (0.40 mL), and dimethylacetamide (2.0 mL) was stirred at 112 °C for 14 h. After cooling, the mixture was poured into ice water (50 mL). The resulting solid was collected by vacuum filtration and purified by flash silica gel column chromatography to give ethyl 2-((5*S*,9*R*)-9-(4-cyanophenyl)-3-(3,5-dichlorophenyl)-1-methyl-2,4-dioxo-1,3,7-triazaspiro[4.4]nonan-7-yl)oxazole-4-carboxylate as yellow solid (0.108 g, 41%). HPLC purity 99%; t_r = 3.55 min (method D). LCMS (EI) m/z Calcd for $C_{26}H_{21}Cl_2N_5O_5$ $[M + H]^+$ 554.10. Found: 554.14. ¹H NMR (500 MHz, CDCl₃) δ 1.36 (3H, t, J = 7.12 Hz), 3.21 (s, 3H), 3.93 (dd, J = 11.70, 7.63 Hz, 1H), 3.99–4.12 (m, 2H), 4.18–4.26 (m, 1H), 4.32–4.46 (m, 3H), 6.74 (d, J = 2.03 Hz, 2H), 7.27–7.29 (m, 1H), 7.33 (d, J = 8.14 Hz, 2H), 7.68 (d, J = 8.65 Hz, 2H), and 7.87 (s, 1H).

To a solution of ethyl 2-((5*S*,9*R*)-9-(4-cyanophenyl)-3-(3,5-dichlorophenyl)-1-methyl-2,4-dioxo-1,3,7-triazaspiro[4.4]nonan-7-yl)oxazole-4-carboxylate (0.060 g, 0.108 mmol) in tetrahydrofuran (2.0 mL) and water (1.0 mL) was added 1,2-propanediol (0.016 mg, 0.216 mmol) followed by a 1*N* aqueous solution of potassium hydroxide (0.270 mL, 0.270 mmol). The mixture was stirred at room temperature for 2.5 h. The mixture was concentrated under reduced pressure, and the pH of the aqueous residue was adjusted to ~5 with acetic acid. The mixture was purified by preparative HPLC to provide **2q** as off-white solid (0.016 g, 28%). HPLC purity 98.5%; t_r = 13.69 min (method A); 98.5%; t_r = 13.33 min (method B). LCMS (EI) m/z Calcd for $C_{24}H_{17}Cl_2N_5O$ $[M + H]^+$ 526.07. Found: 526.16. ¹H NMR (500 MHz, CDCl₃) δ 3.23 (s, 3H), 3.91–4.15 (m, 3H), 4.23 (d, J = 2.75 Hz, 1H), 4.43 (s, 1H), 6.76 (s, 3H), 7.29 (s, 1H), 7.34 (d, J = 7.70 Hz, 2H), 7.69 (d, J = 7.15 Hz, 2H), and 7.96 (s, 1H).

2-((5*S*,9*R*)-9-(4-Cyanophenyl)-3-(3,5-dichlorophenyl)-1-methyl-2,4-dioxo-1,3,7-triazaspiro[4.4]nonan-7-yl)benzo[d]oxazole-7-carboxylic Acid (2r**)**. To a solution of **6** (0.102 g, 0.246 mmol) and methyl 2-chlorobenzo[d]oxazole-7-carboxylate¹⁷ (0.055 g, 0.246 mmol) in anhydrous dimethylformamide (1.5 mL) was added diisopropylethylamine (0.128 mL, 0.738 mmol). The reaction mixture was stirred at 100 °C for 1 h, diluted with water, and extracted with diethyl ether. The organic layer was collected and dried under reduced pressure to give methyl

2-((5*S*,9*R*)-9-(4-cyanophenyl)-3-(3,5-dichlorophenyl)-1-methyl-2,4-dioxo-1,3,7-triazaspiro[4.4]nonan-7-yl)benzo[d]oxazole-7-carboxylate (0.078 g, 54%). HPLC t_r = 3.83 min (method G). LCMS (EI) m/z Calcd for $C_{29}H_{21}Cl_2N_5O_5$ [M + H]⁺ 590.10. Found: 590⁺. ¹H NMR (500 MHz, CDCl₃) δ 3.21 (s, 3H), 3.92 (s, 3H), 4.02 (m, 1H), 4.27 (m, 2H), 4.45 (m, 1H), 4.55 (m, 1H), 6.72 (d, J = 1.65 Hz, 2H), 7.24 (m, 2H), 7.32 (d, J = 8.25 Hz, 2H), 7.58 (d, J = 8.25 Hz, 1H), 7.64 (d, J = 8.25 Hz, 2H), and 7.67 (d, J = 8.25 Hz, 1H).

To a solution of methyl 2-((5*S*,9*R*)-9-(4-cyanophenyl)-3-(3,5-dichlorophenyl)-1-methyl-2,4-dioxo-1,3,7-triazaspiro[4.4]nonan-7-yl)benzo[d]oxazole-7-carboxylate (0.075 g, 0.127 mmol) in anhydrous tetrahydrofuran (4.0 mL) and water (2.0 mL) was added 1,2-propanediol (0.171 mL) and 1.0 M aqueous potassium hydroxide (0.302 mL). After stirring at room temperature for 16 h, the reaction mixture was concentrated under reduced pressure, and the resulting residue was purified by preparative HPLC followed by neutralization with an ion-exchange resin to give **2r** (22.4 mg, 31%) as a white solid. HPLC purity 98.8%; t_r = 14.37 min (method A); 98.7%; t_r = 13.81 min (method B). LCMS (EI) m/z Calcd for $C_{28}H_{19}C_{12}N_5O_5$ [M + H]⁺ 576.08. Found: 576⁺. ¹H NMR (500 MHz, DMSO- d_6) δ 3.19 (s, 3H), 4.10–4.34 (m, 5H), 6.81 (m, 2H), 7.22 (m, 1H), 7.48 (m, 4H), 7.64 (s, 1H), and 7.88 (d, J = 8.0 Hz, 2H).

2-((5*S*,9*R*)-9-(4-Cyanophenyl)-3-(3,5-dichlorophenyl)-1-methyl-2,4-dioxo-1,3,7-triazaspiro[4.4]nonan-7-yl)benzo[d]oxazole-6-carboxylic Acid (2s). To a solution of **6** (0.102 g, 0.246 mmol) and methyl 2-chlorobenzo[d]oxazole-6-carboxylate¹⁷ (0.055 g, 0.246 mmol) in anhydrous dimethylformamide (1.5 mL) was added diisopropylethylamine (0.128 mL, 0.738 mmol). The reaction mixture was stirred at 100 °C for 1 h, diluted with water, and extracted with diethyl ether. The organic layer was collected and dried under reduced pressure to give methyl 2-((5*S*,9*R*)-9-(4-cyanophenyl)-3-(3,5-dichlorophenyl)-1-methyl-2,4-dioxo-1,3,7-triazaspiro[4.4]nonan-7-yl)benzo[d]oxazole-6-carboxylate (0.140 g, 97%). HPLC t_r = 3.86 min (method G). LCMS (EI) m/z Calcd for $C_{29}H_{21}Cl_2N_5O_5$ [M + H]⁺ 590.10. Found: 590⁺. ¹H NMR (500 MHz, CDCl₃) δ 3.26 (s, 3H), 3.90 (s, 3H), 4.33 (m, 2H), 4.60 (m, 3H), 6.73 (s, 2H), 7.19 (s, 1H), 7.28 (d, J = 8.0 Hz, 2H), 7.40 (d, J = 8.0 Hz, 1H), 7.62 (d, J = 8.0 Hz, 2H), 7.90 (d, J = 8.0 Hz, 1H), and 8.00 (s, 1H).

To a solution of methyl 2-((5*S*,9*R*)-9-(4-cyanophenyl)-3-(3,5-dichlorophenyl)-1-methyl-2,4-dioxo-1,3,7-triazaspiro[4.4]nonan-7-yl)benzo[d]oxazole-6-carboxylate (0.140 g, 0.237 mmol) in anhydrous tetrahydrofuran (11.5 mL) and water (5.75 mL) was added 1,2-propanediol (0.684 mL) and 1.0 M aqueous potassium hydroxide (0.603 mL). After stirring at room temperature for 16 h, the reaction mixture was concentrated under reduced pressure, and the resulting residue was purified by preparative HPLC followed by neutralization with ion-exchange resin to provide **2s** (11.6 mg, 8.5%) as a white solid. HPLC purity 94.5%; t_r = 11.50 min (method A; column: SunFire C18 3.5 μ 3.0 mm \times 150 mm); 94.5%; t_r = 11.06 min (method B; column: Xbridge Ph 3.5 μ 3.0 mm \times 150 mm); LCMS (EI) m/z Calcd for $C_{28}H_{19}C_{12}N_5O_5$ [M + H]⁺ 576.08. Found: 576⁺. ¹H NMR (500 MHz, DMSO- d_6) δ 3.19 (s, 3H), 4.17 (m, 1H), 4.28 (m, 2H), 4.38 (m, 2H), 6.80 (m, 2H), 7.40 (d, J = 8.25 Hz, 1H), 7.48 (d, J = 8.25 Hz, 2H), 7.65 (m, 1H), 7.86 (m, 1H), 7.89 (d, J = 8.25 Hz, 2H), and 7.93 (s, 1H).

2-((5*S*,9*R*)-9-(4-Cyanophenyl)-3-(3,5-dichlorophenyl)-1-methyl-2,4-dioxo-1,3,7-triazaspiro[4.4]nonan-7-yl)benzo[d]oxazole-5-carboxylic Acid (2t). To a solution of **6** (0.106 g, 0.256 mmol) and methyl 2-chlorobenzo[d]oxazole-5-carboxylate¹⁷ (0.055 g, 0.256 mmol) in anhydrous dimethylformamide (1.5 mL) was added diisopropylethylamine (0.134 mL, 0.768 mmol). The reaction mixture was stirred at 100 °C for 1 h, diluted with water, extracted with diethyl ether, and dried under reduced pressure. The resulting residue was purified by flash silica gel chromatography using a 97:3 mixture of dichloromethane and methanol to give methyl 2-((5*S*,9*R*)-9-(4-cyanophenyl)-3-(3,5-dichlorophenyl)-1-methyl-2,4-dioxo-1,3,7-triazaspiro[4.4]nonan-7-yl)benzo[d]oxazole-5-carboxylate (0.083 g, 55%). HPLC t_r = 3.76 min (method G).

LCMS (EI) m/z Calcd for $C_{29}H_{21}Cl_2N_5O_5$ [M + H]⁺ 590.10. Found: 590⁺. ¹H NMR (500 MHz, CDCl₃) δ 3.26 (s, 3H), 3.92 (s, 3H), 4.13–4.60 (m, 5H), 6.76 (m, 2H), 7.29 (s, 1H), 7.34 (m, 3H), 7.68 (d, J = 7.2 Hz, 2H), 7.80 (d, J = 8.0 Hz, 1H), and 8.07 (s, 1H).

To a solution of methyl 2-((5*S*,9*R*)-9-(4-cyanophenyl)-3-(3,5-dichlorophenyl)-1-methyl-2,4-dioxo-1,3,7-triazaspiro[4.4]nonan-7-yl)benzo[d]oxazole-5-carboxylate (0.080 g, 0.135 mmol) in anhydrous tetrahydrofuran (4.0 mL) and water (2.0 mL) was added 1,2-propanediol (0.182 mL) and 1.0 M aqueous potassium hydroxide (0.322 mL). After stirring at room temperature for 16 h, the reaction mixture was concentrated under reduced pressure, and the resulting residue was purified by preparative HPLC followed by neutralization with ion-exchange resin to afford **2t** (8.0 mg, 10%) as a white solid. HPLC purity 94.7%; t_r = 7.04 min (method F); 97%; t_r = 3.53 min (method E). LCMS (EI) m/z Calcd for $C_{28}H_{19}C_{12}N_5O_5$ [M + H]⁺ 576.08. Found: 576⁺. ¹H NMR (500 MHz, DMSO- d_6) δ 3.12 (s, 3H), 4.08 (m, 1H), 4.19 (m, 2H), 4.31 (m, 2H), 6.73 (m, 2H), 7.41 (d, J = 8.25 Hz, 2H), 7.46 (d, J = 8.25 Hz, 1H), 7.58 (m, 1H), 7.64 (d, J = 8.25 Hz, 1H), 7.77 (m, 1H), and 7.82 (d, J = 7.7 Hz, 2H).

2-((5*S*,9*R*)-9-(4-Cyanophenyl)-3-(3,5-dichlorophenyl)-1-methyl-2,4-dioxo-1,3,7-triazaspiro[4.4]nonan-7-yl)benzo[d]thiazole-7-carboxylic Acid (2u). To copper(II) bromide (0.200 g, 0.860 mmol) in anhydrous acetonitrile (2.0 mL) was added *tert*-butyl nitrite (0.12 mL, 1.08 mmol) at room temperature over a period of 3 min. After stirring for 5 min at room temperature, methyl 2-amino-benzothiazole-7-carboxylate (0.150 g, 0.720 mmol) was added, and the reaction mixture was heated at 70 °C for 2 h. The reaction mixture was cooled, concentrated under reduced pressure, diluted with ethyl acetate (10 mL), and filtered over a pad of celite. The filtrate was washed with brine (2 \times 25 mL), dried over sodium sulfate, and concentrated to give methyl 2-bromobenzo[d]thiazole-7-carboxylate as a yellow solid (**25**, 0.036 g). The compound was used without further purification.

Methyl 2-((5*S*,9*R*)-9-(4-cyanophenyl)-3-(3,5-dichlorophenyl)-1-methyl-2,4-dioxo-1,3,7-triazaspiro[4.4]nonan-7-yl)benzo[d]thiazole-7-carboxylate was prepared as described in the preparation of **2o** starting from the spirocyclic pyrrolidine (**6**, 0.045 g, 0.108 mmol) and methyl 2-bromobenzo[d]thiazole-7-carboxylate (**25**) to give the desired product (0.025 g; 31%). HPLC purity 93%; t_r = 4.09 min (method E). LCMS (EI) m/z Calcd for $C_{29}H_{21}Cl_2N_5O_4S$ [M + H]⁺ 606.08. Found: 606⁺. ¹H NMR (400 MHz, CDCl₃) δ 3.27 (s, 3H), 4.01 (s, 3H), 4.03–4.16 (m, 2H), 4.18–4.30 (m, 2H), 4.46–4.56 (m, 1H), 6.79 (d, J = 1.51 Hz, 2H), 7.29–7.32 (m, 1H), 7.39 (m, 3H), 7.44 (2H, t, J = 7.81 Hz, 2H), and 7.84 (dd, J = 14.10, 8.06 Hz, 2H).

To methyl 2-((5*S*,9*R*)-9-(4-cyanophenyl)-3-(3,5-dichlorophenyl)-1-methyl-2,4-dioxo-1,3,7-triazaspiro[4.4]nonan-7-yl)benzo[d]thiazole-7-carboxylate (0.013 g, 0.020 mmol) in dimethylformamide (1.0 mL) was added lithium chloride (0.100 g), and the contents were heated at 115 °C for 3 h. The reaction mixture was cooled to room temperature, and acetic acid (3.0 mL) and water (3.0 mL) were added. The resulting precipitate was collected by vacuum filtration and dried in a vacuum oven at 50 °C for 50 h to give **2u** as a white solid (0.011 g; 86%). HPLC purity 97.4%; t_r = 11.51 min (method A; column: SunFire C18 3.5 μ 3.0 mm \times 150 mm); 96.5%; t_r = 11.22 min (method B; column: Xbridge Ph 3.5 μ 3.0 mm \times 150 mm). LCMS (EI) m/z Calcd for $C_{28}H_{19}C_{12}N_5O_4S$ [M + H]⁺ 592.06. Found: 592⁺. ¹H NMR (400 MHz, DMSO- d_6) δ 3.23 (s, 3H), 4.11–4.40 (m, 4H), 4.41–4.55 (m, 1H), 6.75–6.88 (m, J = 1.51 Hz, 2H), 7.41–7.55 (m, 3H), 7.64–7.69 (m, 1H), 7.75 (dd, J = 12.34, 7.30 Hz, 2H), and 7.91 (d, J = 8.06 Hz, 2H).

2-((5*S*,9*R*)-9-(4-Cyanophenyl)-3-(3,5-dichlorophenyl)-1-methyl-2,4-dioxo-1,3,7-triazaspiro[4.4]nonan-7-yl)benzo[d]thiazole-6-carboxylic Acid (2v). A mixture of **6** (0.100 g, 0.241 mol), methyl 2-bromobenzo[d]thiazole-6-carboxylate (0.072 g, 0.265 mmol), and diisopropylamine (0.084 mL, 0.482 mmol) in anhydrous dimethylformamide (3.0 mL) was heated at 100 °C overnight.

The reaction mixture was cooled to room temperature, and water was added until a precipitate formed. The solid was collected by vacuum filtration, washed with water, and dried to give a tan solid. Purification by flash silica gel chromatography afforded methyl 2-((5*S*,9*R*)-9-(4-cyanophenyl)-3-(3,5-dichlorophenyl)-1-methyl-2,4-dioxo-1,3,7-triazaspiro[4.4]nonan-7-yl)benzo[d]thiazole-6-carboxylate (0.064 g) as an off-white solid. HPLC purity 98%; $t_r = 3.64$ min (method D). LCMS (EI) m/z Calcd for $C_{29}H_{21}Cl_2N_5O_4S$ [M + H]⁺ 606.08. Found: 606.39 and 608.30. ¹H NMR (500 MHz, CDCl₃) δ 2.06 (s, 3H), 2.97 (s, 3H), 4.18 (d, $J = 11.6$ Hz, 1H), 4.28 (t, $J = 13.8$ Hz, 1H), 4.35–4.37 (m, 3H), 7.20 (s, 2H), 7.34–7.36 (m, 3H), 7.63 (d, $J = 8.25$ Hz, 1H), 7.69 (d, $J = 8.25$ Hz, 2H), 8.10 (d, $J = 9.35$ Hz, 1H), and 8.43 (s, 1H).

A mixture of methyl 2-((5*S*,9*R*)-9-(4-cyanophenyl)-3-(3,5-dichlorophenyl)-1-methyl-2,4-dioxo-1,3,7-triazaspiro[4.4]nonan-7-yl)benzo[d]thiazole-6-carboxylate (0.037 g, 0.061 mmol) and lithium iodide (0.250 g) in anhydrous dimethylacetamide (1.0 mL) was heated at 140 °C overnight. The reaction was cooled to room temperature, and acetic acid (~12 drops from a pipet) was added followed by water (3.0 mL). The dimethylformamide was removed under reduced pressure, and the resulting residue was purified by preparative HPLC to give **2v** (14 mg) as a white solid. HPLC purity 96.6%; $t_r = 14.69$ min (method A); 96.7%; $t_r = 14.17$ min (method B). LCMS (EI) m/z Calcd for $C_{28}H_{19}Cl_2N_5O_4S$ [M + H]⁺ 592.06. Found: 592.09 and 594.07. ¹H NMR (500 MHz, DMSO-*d*₆) δ 3.26 (s, 3H), 4.03–4.25 (m, 4H), 4.50 (t, $J = 10.72$ Hz, 1H), 6.79 (s, 2H), 7.29 (s, 1H), 7.37 (d, $J = 8.25$ Hz, 2H), 7.65 (d, $J = 8.25$ Hz, 1H), 7.69 (d, $J = 7.70$ Hz, 2H), 8.09 (d, $J = 8.80$ Hz, 1H), and 8.40 (s, 1H).

4-((5*S*,9*R*)-3-(3,5-Dichlorophenyl)-1-methyl-2,4-dioxo-1,3,7-triazaspiro[4.4]nonan-9-yl)benzotrile (6). The detailed procedure for the preparation of **6** is outlined in refs 6b and 11. The retention times on the Chiralpak-AD column and specific rotations for these compounds are as follows: enantiomeric excess > 99%; $t_R = 5.74$ min [Chiralpak-AD column (7.5 cm × 30 cm) under SFC conditions (70% CO₂/30% MeOH)]; specific rotation: $[\alpha]_D^{25} = +95.2$ ($c = 1$, MeOH).

HUVEC: Human T-Cell Adhesion Assay. PBMCs were isolated from human peripheral blood and T cells expanded with phytohemagglutinin (PHA). HUVEC were obtained from Clonetics (San Diego, CA), grown to confluence in 96-well plates and stimulated overnight with PMA to increase ICAM-1 expression. PHA blasts were labeled with calcein-AM according to the manufacturer's instructions (Invitrogen, Carlsbad, CA) and treated with PMA to increase LFA-1 avidity. PHA blasts were then added to the activated HUVEC monolayer in the presence or absence of compound or an excess of anti-LFA-1 antibody. The monolayers were washed and adhesion of calcein-labeled cells was determined by reading plates on a Cytofluor (fluorescence plate reader; excitation 485/emission 530 nm). Adhesion in the presence of vehicle control was considered equivalent to 0% inhibition. Adhesion in the presence of an excess of antihuman LFA-1 antibody was considered equivalent to 100% inhibition.

b.END3 Mouse T-Cell Adhesion Assay. Given the observation that mouse LFA-1 fails to recognize human ICAM-1¹⁸ combined with the observations of others that some LFA-1 antagonists demonstrate a preference for human LFA-1 versus mouse LFA-1,^{9a} a mouse adhesion assay was established to identify compounds appropriate for in vivo evaluation. Adhesion of the murine T-cells to mTNF α -activated monolayers of the mouse b.END3 cell line was used for the mouse cell–cell adhesion assay. Splenocytes were isolated from C57BL/6 mice and grown for 4 d on anti-CD3 (145–2C11)/anti-CD28 (3N7)-coated plates. The T-cells were then transferred to uncoated plates and grown overnight in IL-2-containing media. Prior to adhesion assays, the expanded mouse T-cells were harvested, resuspended in HBSS, labeled with calcein-AM, and then treated with PMA to increase the avidity of LFA-1. These activated, calcein-labeled T-cells were then added to a monolayer of

TNF α -activated b.END3 cells in the presence or absence of BMS-688521 or antimouse LFA-1 Ab. The monolayers were washed, and adhesion of calcein-labeled T-cells was determined by reading plates on a Cytofluor. Adhesion in the presence of vehicle alone was considered equivalent to 0% inhibition. Adhesion in the presence of an excess (10 μ g/mL) of antimouse LFA-1 Ab (M17) was considered equivalent to 100% inhibition.

Human Mixed Lymphocyte Reaction (MLR) Assay. Peripheral blood mononuclear cells (PBMC) were obtained by density-gradient separation (Lymphocyte Separation Media; Mediatech Inc., Herndon, VA) of EDTA-treated whole blood from normal healthy donors. T-cells were prepared from E⁺ fractions of PBMC rosetted with sheep red blood cells (SRBC, Colorado Serum Company; Denver, CO). T-cells were cultured at 1×10^5 cells/well in quadruplicate wells together with 1×10^5 of irradiated allogeneic PBMCs as antigen-presenting cells (APCs) in 96-well round-bottom plates in a total volume of 200 μ L of 10% FCS-RPMI. Compounds were added to the cell mixture at the initiation of the response. On day 4 after initiation of the MLR, cultures were pulsed with one μ Ci of ³[H]-thymidine (PerkinElmer, Boston, MA) for 6 h, harvested on a Packard cell harvester (PerkinElmer), and counted by liquid scintillation on a Packard TopCount NXT (PerkinElmer). Proliferation was determined by incorporation of the ³H label into DNA.

Human Whole-Blood IL-2 mRNA Determination. A whole blood IL-2 mRNA assay was used to further characterize compound **2e**. The IL-2 assay was conducted on heparinized whole blood that had been activated with SEB. This response can be blocked with anti-LFA-1 antibody, demonstrating that SEB-induced IL-2 mRNA production is LFA-1-dependent. For this assay, total RNA was isolated from whole blood leukocytes at 6 h post SEB-induced activation by using the QIAamp RNA Blood Mini Kit (Qiagen, Valencia, CA) according to the manufacturer's instructions. The IL-2 mRNA was quantified by real-time polymerase chain reaction (RT-PCR) using SYBR Green I reagent (Applied Biosystems, Foster City, CA) (30), and GAPDH mRNA as an internal standard. Specifically, 500 ng of RNA was used to make cDNA using SuperScript II RNase H (Invitrogen, Carlsbad CA) reverse transcriptase with oligo (dT)_{12–18} primer (Invitrogen, Carlsbad CA). IL-2 message was detected with the forward primer CTGCTGGATTTACAGATGATTTTGA and the reverse primer TTGGGCATGTAAAACCTTAAATGTGA. The primers used to detect GAPDH message were AATTC-CATGGCACCCTCAAG (forward primer) and GAAGACGC-CAGT-GGACTCCA (reverse primer). IC₅₀ values were calculated using the $\Delta\Delta C_T$ method to determine relative IL-2 mRNA levels.

OVA Lung Inflammation in Mice. BALB/c female mice, 6–8 week of age, (Harlan, Indianapolis, IN) were immunized intraperitoneally with 100 μ g of ovalbumin (OVA; Sigma) in alum adjuvant (Pierce) and similarly boosted 14 days later. Fourteen days after the booster, the mice were challenged intranasally with 100 μ g OVA in 50 μ L of pyrogen-free saline. Seventy-two hours after challenge, mice were killed by barbiturate overdose, and the lungs were lavaged via a tracheostomy with 1 mL of ice-cold Hank's balanced salt solution (Ca⁺⁺- and Mg⁺⁺-free) containing 10% fetal bovine serum. Total recovered leukocytes were enumerated by electronic cell counter (Scharfe System, Reutigen, Germany). Cytocentrifuge smears (Shandon, Pittsburgh) were stained with Wright's Giemsa stain, and 200 cells per sample were classified by microscopic differential.

X-ray Crystallography. The I-Domain of LFA-1 was incubated overnight at 4 °C with a 2.1 molar excess of ligand. Crystals were grown by hanging drop vapor diffusion with a drop consisting of 1 μ L of protein/ligand solution and 1 μ L of reservoir solution, which contained 0.1 M sodium citrate, pH 5.6, 80% (v/v) saturated sodium citrate, which was not titrated, and 3% (v/v) ethylene glycol. The crystal was prepared for flash cooling by placing the crystal in a solution consisting 80% reservoir solution and 20% ethylene glycol and then plunging the looped crystal into liquid nitrogen. Data were collected using a Rigaku FR-E

Table 7. X-ray Crystallography Data Collection and Refinement Statistics

space group	$P2_12_12_1$	
a , Å	40.6	
b , Å	63.6	
c , Å	63.1	
	overall	last
resolution, Å	50–1.85	1.92–1.85
measured	91910	≥6398
unique	13552	1089
redundancy	6.8	6.6
% complete	93.3	76.8
R value	0.86	0.310
I/σ_1	23.0	5.8
R_{work}	0.192	
R_{free}	0.227	
rmsd bond distances, Å	0.006	
rmsd bond angles, deg	1.1	

equipped with MicroMax optics and a Rigaku Saturn92 detector. The data was processed with HKL2000¹⁹ and had symmetry consistent with space group $P2_12_12_1$ and unit cell parameters of $a = 40.6$ Å, $b = 63.6$ Å, and $c = 63.1$ Å (the inverted distance order of the b and c axes kept the same indexing as a canonical data set where the c axis was longer than the b axis). A cycle of rigid body fitting was carried out with the CCP4 version of AMoRe.²⁰ Refinement was performed with CNX²¹ starting with a cycle of rigid body refinement and followed by an annealing protocol and individual B-factor refinement. QUANTA²² was used for examining the model and the electron density maps. The ligand was placed by the X-ligand module of QUANTA,²² and water molecules were placed by examination. Electron density map fitting was alternated with refinement of the model with CNX using only minimization and individual B factor refinement until no significant electron density was uninterpreted. The final R_{work} was 0.219 and R_{free} was 0.255. The rmsd for bond distances was 0.007 Å and the rmsd for bond angles was 1.4° (Table 7).

References

- (1) (a) Hogg, N.; Henderson, R.; Leitinger, B.; McDowall, A.; Porter, J.; Stanley, P. Mechanisms contributing to the activity of integrins on leukocytes. *Immunol. Rev.* **2002**, *186*, 164–171. (b) Smith, A.; Stanley, P.; Jones, K.; Svensson, L.; McDowall, A.; Hogg, N. The role of the integrin LFA-1 in T-lymphocyte migration. *Immunol. Rev.* **2007**, *218*, 135–146. (c) Welzenbach, K.; Hommel, U.; Weitz-Schmidt, G. Small molecule inhibitors induce conformational changes in the I Domain and the I-like domain of lymphocyte function-associated antigen-1. *J. Biol. Chem.* **2002**, *277*, 10590–10598.
- (2) (a) Shimaoka, M.; Springer, T. A. Therapeutic antagonists and the conformational regulation of the β_2 integrins. *Curr. Top. Med. Chem.* **2004**, *4*, 1485–1495. (b) Shimaoka, M.; Xiao, T.; Liu, J.-H.; Yang, Y.; Dong, Y.; Jun, C.-D.; McCormick, A.; Zhang, R.; Joachimak, A.; Takagi, J.; Wang, J.-H.; Springer, T. A. Structures of the α L I Domain and its complex with ICAM-1 reveal a shape-shifting pathway for integrin regulation. *Cell* **2003**, *112*, 99–111. (c) Ma, Q.; Shimaoka, M.; Lu, C.; Jing, H.; Carman, C. V.; Springer, T. A. Activation-induced conformational changes in the I Domain region of lymphocyte function-associated antigen-1. *J. Biol. Chem.* **2002**, *277*, 10638–10641. (d) Salas, A.; Shimaoka, M.; Chen, S.; Carman, C. V.; Springer, T. Transition from rolling to firm adhesion is regulated by the conformation of the I Domain of the integrin lymphocyte function-associated antigen-1. *J. Biol. Chem.* **2002**, *277*, 50255–50262. (e) Takagi, J.; Springer, T. A. Integrin activation and structural rearrangement. *Immunol. Rev.* **2002**, *186*, 141–163.
- (3) Berlin-Rufenach, C.; Otto, F.; Mathies, M.; Westermann, J.; Owen, M. J.; Hamann, A.; Hogg, N. Lymphocyte Migration in Lymphocyte Function-Associated Antigen (LFA)-1-deficient Mice. *J. Exp. Med.* **1999**, *189*, 1467–1478.
- (4) (a) Selenko-Gebauer, N.; Karhofer, F.; Stingl, G. Efalizumab in routine use: a clinical experience. *Br. J. Dermatol.* **2007**, *156*, 1–6. (b) Lebwohl, M.; Tying, S. K.; Hamilton, T. K.; Toth, D.; Glazer, S.; Tawfik, N. H.; Walicke, P.; Dummer, W.; Wang, X.; Garovoy, M. R.; Pariser, D. A novel targeted T-cell modulator, Efalizumab, for plaque psoriasis. *N. Engl. J. Med.* **2003**, *349*, 2004–2013. (c) Cather, J. C.; Cather, J. C.; Menter, A. Modulating T cell responses for the treatment of psoriasis: a focus on Efalizumab. *Expert Opin. Biol. Ther.* **2003**, *3*, 361–370. (d) Dedrick, R. L.; Walicke, P.; Garovoy, M. Anti-adhesion antibodies Efalizumab, a humanized anti-CD11a monoclonal antibody. *Transplant Immunol.* **2002**, *9*, 181–186.
- (5) Liu, G. Inhibitors of LFA-1/ICAM-1 interaction: From monoclonal antibodies to small molecules. *Drugs Future* **2001**, *26*, 767–778 and references cited therein.
- (6) Dodd, D. S.; Sheriff, S.; Chang, C.-Y. J.; Stetsko, D. K.; Phillips, L. M.; Zhang, Y.; Launay, M.; Potin, D.; Varcarrro, W.; Poss, M. A.; McKinnon, M.; Barrish, J. C.; Suchard, S. J.; Dhar, T. G. M. Design of LFA-1 agonists based on a 2,3-dihydro-1H-pyrrolizin-5(7aH)-one scaffold. *Bioorg. Med. Chem. Lett.* **2007**, *17*, 1908–1911. (b) Potin, D.; Launay, M.; Monatlif, F.; Malabre, P.; Fabreguette, M.; Fouquet, A.; Maillet, M.; Nicolai, E.; Dorgeret, L.; Chevallier, F.; Besse, D.; Dufort, M.; Caussade, F.; Ahmad, S. Z.; Stetsko, D. K.; Skala, S.; Davis, P. M.; Balimane, P.; Patel, K.; Yang, Z.; Marathe, P.; Postelneck, J.; Townsend, R. M.; Goldfarb, W.; Sherriff, S.; Einspahr, H.; Kish, K.; Malley, M. F.; DiMarco, J. D.; Gougoutas, J. Z.; Kadiyala, P.; Cheney, D. L.; Tejwani, R. W.; Murphy, D. K.; McIntyre, K. W.; Yang, X.; Chao, S.; Leith, L.; Xiao, Z.; Mathur, A.; Chen, B.-C.; Wu, D.-R.; Traeger, S. C.; McKinnon, M.; Barrish, J. C.; Robl, J. A.; Iwanowicz, E. J.; Suchard, S. J.; Dhar, T. G. M. Discovery and Development of 5-[(5S,9R)-9-(4-Cyanophenyl)-3-(3,5-dichlorophenyl)-1-methyl-2,4-dioxo-1,3,7-triazaspiro [4.4]non-7-yl]methyl]-3-thiophenecarboxylic acid (BMS-587101)—A small molecule antagonist of leukocyte function associated antigen-1. *J. Med. Chem.* **2006**, *49*, 6946–6949. (c) Potin, D.; Launay, M.; Nicolai, E.; Fabreguette, M.; Malabre, P.; Caussade, F.; Besse, D.; Skala, S.; Stetsko, D. K.; Todderud, G.; Beno, B. R.; Cheney, D. L.; Chang, C. J.; Sheriff, S.; Hollenbaugh, D. L.; Barrish, J. C.; Iwanowicz, E. J.; Suchard, S. J.; Dhar, T. G. M. De novo design, synthesis and in vitro activity of LFA-1 antagonists based on a bicyclic[5.5]hydantoin scaffold. *Biorg. Med. Chem. Lett.* **2005**, *15*, 1161–1164.
- (7) (a) Wattanasin, S.; Kallen, J.; Myers, S.; Guo, Q.; Sabio, M.; Ehrhardt, C.; Albert, R.; Hommel, U.; Weckbecker, G.; Welzenbach, K.; Weitz-Schmidt, G. 1,4-Diazepane-2,5-diones as novel inhibitors of LFA-1. *Bioorg. Med. Chem. Lett.* **2005**, *15*, 1217–1220. (b) Wu, J.-P.; Erneigh, J.; Gao, A. A.; Goldberg, D. R.; Kuzmich, D.; Miao, C.; Potocki, I.; Qian, K. C.; Sorcek, R. J.; Jeanfavre, D. D.; Kishimoto, K.; Mainolfi, E. A.; Nabozny, G.; Peng, C.; Reilly, P.; Rothlein, R.; Sellati, R. H.; Woska, J. R.; Chen, S.; Gunn, J. A.; O'Brien, D.; Norris, S. H.; Kelly, T. A. Second-generation lymphocyte function-associated antigen-1 inhibitors: 1H-Imidazo[1,2-a]imidazol-2-one derivatives. *J. Med. Chem.* **2004**, *47*, 5356–5366. (c) Gadek, T. R.; Burdick, D. J.; McDowell, R. S.; Stanley, M. S.; Marsters, J. C., Jr.; Paris, K. J.; Oare, D. A.; Reynolds, M. E.; Ladner, C.; Zioncheck, K. A.; Lee, W. P.; Gribling, P.; Dennis, M. S.; Skelton, N. J.; Tumas, D. B.; Claark, K. R.; Keating, S. M.; Beresini, M. H.; Tilley, J. W.; Presta, L. G.; Bodary, S. C. Generation of an LFA-1 antagonist by the transfer of ICAM-1 immunoregulatory epitope to a small molecule. *Science* **2002**, *295*, 1086–1089. (d) Sircar I.; Furth, P.; Teegarden, B. R.; Moringstar, M.; Smith, N.; Griffith, R. Patent WO 0130781 (Tanabe Seiyaku) 2001. (e) Weitz-Schmidt, G.; Welzenbach, K.; Brinkmann, V.; Kamata, T.; Kallen, J.; Bruns, C.; Cottens, S.; Takada, Y.; Hommel, U. Statins selectively inhibit leukocyte function antigen-1 by binding to a novel regulatory integrin site. *Nat. Med.* **2001**, *7*, 687–692. (f) Kelly, T. A.; Jeanfavre, D. D.; McNeil, D. W.; Woska, R. J.; Reilly, L. P.; Mainolfi, E. A.; Kishimoto, K. M.; Nabozny, G. H.; Zinter, R.; Bormann, B.; Rothlein, R. Cutting edge: A small molecule antagonist of LFA-1 mediated cell adhesion. *J. Immunol.* **1999**, *163*, 5173–5177.
- (8) Last-Barney, K.; Davidson, W.; Cardozo, M.; Frye, L. L.; Grygon, C. A.; Hopkins, J. L.; Jeanfavre, D. D.; Pav, S.; Qian, C.; Stevenson, J. M.; Tong, L.; Zindell, R.; Kelly, T. A. Binding site elucidation of hydantoin-based antagonists of LFA-1 using multidisciplinary techniques: Evidence for the allosteric inhibition of a protein–protein interaction. *J. Am. Chem. Soc.* **2001**, *125*, 5643–5650.
- (9) Similar results were seen with a Boehringer–Ingelheim series of LFA-1 antagonists. (a) Winquist, R. J.; Desai, S.; Fogal, S.; Haynes, N. A.; Nabozny, G. H.; Reilly, P. L.; Souza, D.; Panzenbeck, M. The role of leukocyte function-associated antigen-1 in animal models of inflammation. *Eur. J. Pharmacol.* **2001**, *429*, 297–302. (b) Panzenbeck, M. J.; Jeanfavre, D. D.; Kelly, T. A.; Lemieux, R.; Nabozny, G.; Reilly, P. L.; Desai, S. An orally active, primate selective antagonist of LFA-1 inhibits delayed-type hypersensitivity in a humanized-mouse model. *Eur. J. Pharmacol.* **2006**, *534*, 233–240.
- (10) Sushard, S. J.; Stetsko, D. K.; Davis, P. M.; Skala, S.; Potin, D.; Launay, M.; Dhar, T. G. M.; Barrish, J. C.; Susulic, V.; Shuster, D. J.; McIntyre, K. W.; McKinnon, M.; Salter-Cid, L. An LFA-1 ($\alpha_L\beta_2$) small-molecule antagonist reduces inflammation and joint destruction in murine models of arthritis. *J. Immunol.* **2010**, *184*, 3917–3926.
- (11) Dhar, T. G. M.; Launay, M.; Potin, D.; Watterson, S. H.; Xiao, Z. Pyridyl-substituted spiro-hydantoin compounds and their preparation,

- pharmaceutical compositions and use for treatment of immune and inflammatory diseases. US 7186727 2007; *Chem. Abstr.* **2006**, 145, 83333.
- (12) Jiang, L.; Buchwald, S. L. Palladium catalyzed aromatic carbon-nitrogen bond formation. In *Metal-Catalyzed Cross-Coupling Reactions*, 2nd ed.; De Meijere, A., Diederich, F., Eds.; Wiley-VCH: Weinheim, Germany, 2004; pp 699–760.
- (13) Chan, D. M. T.; Monaco, K. L.; Li, R.; Bonne, D.; Clark, C. G.; Lam, P. Y. S. Copper promoted C–N and C–O bond cross-coupling with phenyl and pyridylboronates. *Tetrahedron Lett.* **2003**, 44, 3863–3865.
- (14) (a) Ohta, K.; Kawachi, E.; Inoue, N.; Fukasawa, H.; Hashimoto, Y.; Itai, A.; Kagechika, H. Retinoidal pyrimidinecarboxylic acids. Unexpected diaza-substituent effects in retinobenzoic acids. *Chem. Pharm. Bull.* **2000**, 48, 1504–1513. (b) Takamizawa, A.; Hirai, K. Pyrimidine derivatives, XXXI. Reactions of ethyl 2-methoxy-methylene-3-ethoxypropionate with ureas. *Chem. Pharm. Bull.* **1964**, 12, 804–808.
- (15) (a) McOmie, J. F. W.; White, I. M. Pyrimidines. Part VI. 5-Bromopyrimidine. *J. Chem. Soc.* **1953**, 3129–3131. (b) Kim, C.-H.; Marquez, V. E.; Mao, D. T.; Haines, D. R.; McCormack, J. J. Synthesis of pyrimidine-2-one nucleosides as acid-stable inhibitors of cytidine deaminase. *J. Med. Chem.* **1986**, 29, 1374–1380. (c) Clark, M. P.; Laufersweiler, M. J.; Djung, J. F.; Natchus, M. G.; De, B. Preparation of 3-(pyrimidin-4-yl)-6,7-dihydro-5H-pyrazolo[1,2-a]pyrazol-1-ones for control of inflammatory cytokines. Patent WO 2003024971 A1 20030327, 2003; *Chem. Abstr.* **2003**, 138, 271694.
- (16) (a) Daves, G. D.; Baiocchi, F.; Robins, R. K.; Cheng, C. C. Pyrimidines. II. Orotic acid analogs. *J. Org. Chem.* **1961**, 26, 2755–2763. (b) Daves, G. D.; O'Brien, D. E.; Lewis, L. R.; Cheng, C. C. Pyrimidines. XI. 11. 2- and 6-substituted 4-pyrimidinecarboxylic acids (1a). *J. Heterocycl. Chem.* **1964**, 1, 130–133.
- (17) Lok, R.; Leone, R. E.; Williams, A. J. Facile rearrangements of alkynylamino heterocycles with noble metal cations. *J. Org. Chem.* **1996**, 61, 3289–3297.
- (18) Edwards, C. P.; Champe, M.; Gonzalez, T.; Wessinger, M. E.; Spencer, S. A.; Presta, L. G.; Berman, P. W.; Bodary, S. C. Identification of amino acids in the CD11a I-domain important for binding of the leukocyte function-associated antigen-1 (LFA-1) to intercellular adhesion molecule-1 (ICAM-1). *J. Biol. Chem.* **1995**, 270, 12635–12640.
- (19) Otwinowski, Z.; Minor, W. In *Methods in Enzymology*, Vol. 276: *Macromolecular Crystallography Part A*; Abelson, J. N., Simon, M. I., Carter, C. W., Jr., Sweet, R. M., Eds.; Academic Press: New York 1997; pp 307–326.
- (20) (a) Collaborative Computational Project, Number 4. The CCP4 Suite: programs for protein crystallography. *Acta Crystallogr., Sect. D: Biol. Crystallogr.* **1994**, 50, 760–763. (b) Navaza, J. AMoRe: an automated package for molecular replacement. *Acta Crystallogr., Sect. A: Found. Crystallogr.* **1994**, 50, 157–163.
- (21) *CNX release 2002*; Accelrys, Inc.: San Diego, CA, **2002**.
- (22) *QUANTA Modeling Environment release 2000*; Accelrys Inc.: San Diego, CA, **2000**.